OXFORD UNIVERSITY PRESS | Brain

LGI1 antibodies alter Kv1.1 and AMPA receptors changing synaptic excitability, plasticity and memory

Journal:	*Brain*
Manuscript ID	Draft
Manuscript Type:	Original Article
Date Submitted by the Author:	n/a
Complete List of Authors:	Petit-Pedrol, Mar; Institut d'Investigacions Biomèdiques August Pi i Sunyer (IDIBAPS), Hospital Clínic, Universitat de Barcelona Sell, Josefine; Hans-Berger Department of Neurology; Center for Sepsis Control and Care (CSCC), Jena University Hospital Planagumà, Jesús; Institut d'Investigacions Biomèdiques August Pi i Sunyer (IDIBAPS), Hospital Clínic, Universitat de Barcelona Mannara, Francesco; Institut d'Investigacions Biomèdiques August Pi i Sunyer (IDIBAPS), Hospital Clínic, Universitat de Barcelona Radosevic, Marija; Institut d'Investigacions Biomèdiques August Pi i Sunyer (IDIBAPS), Hospital Clínic, Universitat de Barcelona Haselmann, Holger; Hans-Berger Department of Neurology; Center for Sepsis Control and Care (CSCC), Jena University Hospital Ceanga, Mihai; Hans-Berger Department of Neurology Sabater, Lidia; Institut d'Investigacions Biomèdiques August Pi i Sunyer (IDIBAPS), Hospital Clínic, Universitat de Barcelona Spatola, Marianna; Institut d'Investigacions Biomèdiques August Pi i Sunyer (IDIBAPS), Hospital Clínic, Universitat de Barcelona; University of Lausanne (UNIL) Soto, David; Institut d'Investigacions Biomèdiques August Pi i Sunyer (IDIBAPS), Hospital Clínic, Universitat de Barcelona; Laboratori de Neurofisiologia, Departament de Biomedicina, Facultat de Medicina i Ciències de la Salut, Institut de Neurociències, Universitat de Barcelona Gasull, Xavier; Institut d'Investigacions Biomèdiques August Pi i Sunyer (IDIBAPS), Hospital Clínic, Universitat de Barcelona; Laboratori de Neurofisiologia, Departament de Biomedicina, Facultat de Medicina i Ciències de la Salut, Institut de Neurociències, Universitat de Barcelona Dalmau, Josep; Institut d'Investigacions Biomèdiques August Pi i Sunyer (IDIBAPS), Hospital Clínic, Universitat de Barcelona; Department of Neurology, University of Pennsylvania; Centro de Investigación Biomédica en Red Enfermedades Raras (CIBERER); Institució Catalana de Recerca i Estudis Avançats (ICREA) Geis, Christian; Hans-Berger Department of Neurology; Center for Sepsis Control and Care (CSCC), Jena University Hospital
Subject category:	Multiple sclerosis and neuroinflammation
To search keyword list, use whole or part words followed	Limbic encephalitis < MULTIPLE SCLEROSIS AND NEUROINFLAMMATION, Neuroimmunology < MULTIPLE SCLEROSIS AND NEUROINFLAMMATION,

by an *:	Synaptic transmission < SYSTEMS/DEVELOPMENT/PHYSIOLOGY, Plasticity < SYSTEMS/DEVELOPMENT/PHYSIOLOGY, Memory < DEMENTIA

LGI1 antibodies alter Kv1.1 and AMPA receptors changing synaptic excitability, plasticity and memory

Mar Petit-Pedrol[1,*], Josefine Sell[2,*], Jesús Planagumà[1], Francesco Mannara[1], Marija Radosevic[1], Holger Haselmann[2,3], Mihai Ceanga[2], Lidia Sabater[1], Marianna Spatola[1,4], David Soto[1,5], Xavier Gasull[1,5], Josep Dalmau[1,6,7, 8,$], and Christian Geis[2,3,$]

[1]Institut d'Investigacions Biomèdiques August Pi i Sunyer (IDIBAPS), Hospital Clínic, Universitat de Barcelona, Barcelona, Spain; [2]Hans-Berger Department of Neurology, [3]Center for Sepsis Control and Care (CSCC), Jena University Hospital, Jena, Germany; [4] University of Lausanne (UNIL), Lausanne, Switzerland; [5]Laboratori de Neurofisiologia, Departament de Biomedicina, Facultat de Medicina i Ciències de la Salut, Institut de Neurociències, Universitat de Barcelona, Barcelona, Spain; [6]Department of Neurology, University of Pennsylvania, Philadelphia, USA; [7]Centro de Investigación Biomédica en Red Enfermedades Raras (CIBERER); [8]Institució Catalana de Recerca i Estudis Avançats (ICREA), Barcelona, Spain.

[*]**Contributed equally**

[$]**Share seniority**

Corresponding author: Josep Dalmau, MD, PhD, IDIBAPS-Hospital Clínic, University of Barcelona, Casanova, 143; Floor 3ª, Barcelona 08036 (Spain); Phone: +34 932 271 738 Fax: +34 932 271 726. E-mail: Jdalmau@clinic.cat

Running title: Mechanisms of anti-LGI1 encephalitis

Abstract

Autoimmune encephalitis with antibodies against leucine-rich glioma-inactivated 1 (LGI1) protein is the most frequent form of immune-mediated limbic encephalitis usually presenting with severe impairment in memory formation preceded by faciobrachial dystonic seizures that often respond to immunotherapy. LGI1 is a neuronal secreted synaptic linker protein that connects presynaptic voltage-gated potassium channels Kv1.1 with postsynaptic α-amino-3-hydroxy-5-methyl-4-isoxazolepropionic acid (AMPA) receptors through the interaction with the transmembrane disintegrin and metalloprotease domain family members ADAM23 and 22, respectively. Despite evidence suggesting the disorder is immune-mediated the pathophysiology of how human LGI1 antibodies cause disease symptoms is largely unknown. Here we used highly specific patient-derived immunoglobulin G to determine the main epitope regions, the potential antibody interference of the interaction between LGI1 and ADAM23 and 22, and the effects on behavior, presynaptic Kv1.1 and postsynaptic AMPA receptors, synaptic transmission, and plasticity. Purified immunoglobulin G samples of 25 patients and 20 controls, and experiments with 118 mice including behavioral test, brain tissue analysis with confocal microscopy, and electrophysiology were used in the study. All patients´ samples prevented binding of LGI1 to ADAM23, but only 60% to ADAM22. Using deletion constructs of LGI1 we found obligate binding of patients´ antibodies to the leucine rich repeat domain and less frequent binding to the epitempin domain. Passive cerebroventricular transfer of patients´ immunoglobulin G antibodies to mice led to prolonged but reversible deficits in memory function. Confocal analysis of hippocampal brain slices showed reduced total and synaptic levels of Kv1.1 following the time course of animal memory deficit, with complete recovery 33 days after the end of the infusion. Reduction of AMPA

receptors was present in a time-displaced manner following the loss of Kv1.1. In acute slice preparations of hippocampus, patch-clamp analysis from dentate gyrus granule cells revealed neuronal hyperexcitability with increased glutamatergic transmission and higher presynaptic release probability most likely induced by the reduced expression of Kv1.1. Analysis of synaptic plasticity by recording field potentials in the CA1 region of the hippocampus revealed severely affected long-term potentiation consistent with the memory deficits observed in mice. Different from genetic models of LGI1 deficiency, we did not observe aberrant dendritic sprouting or defective synaptic pruning as major pathology underlying disease symptoms. Overall, these findings reveal several LGI1 antibody-mediated pathogenic mechanisms that interference with LGI1-associated pathways, altering presynaptic and postsynaptic signaling, and resulting in synaptic hyperexcitability, decreased plasticity, and memory deficits.

Keywords

Limbic encephalitis, LGI1, AMPA receptors, Kv1.1, synaptic hyperexcitability

Introduction

Autoimmune encephalitides refer to a group of inflammatory brain diseases that manifest with prominent neuropsychiatric symptoms and are associated with antibodies against neuronal cell surface proteins, ion channels or receptors (Dalmau *et al.*, 2017). One of the most frequent types of autoimmune encephalitis predominantly affects the limbic system (limbic encephalitis) and can result from autoantibodies against different antigens, such as leucine-rich glioma-inactivated 1 (LGI1) protein, the α-amino-3-hydroxy-5-methyl-4-isoxazolepropionic acid receptor (AMPAR), the γ-aminobutyric acid (GABA) type B receptor, or contactin-associated protein‐like 2 (Caspr2), each of

them manifesting with a core syndrome that includes severe difficulty in forming new memories (anterograde or short-term memory deficit), changes of mood and behavior, and variable presence of seizures (Dalmau and Graus, 2018). The most frequent is autoimmune limbic encephalitis with antibodies against LGI1 (Irani *et al.*, 2010; Lai *et al.*, 2010) . Patients with this disorder often present with faciobrachial dystonic seizures or hyponatremia that precede or develop together with the aforementioned core syndrome of limbic dysfunction (Irani *et al.*, 2013). Less frequently, patients with LGI1 antibodies present with rapidly progressive dementia which, as the other clinical manifestations, is responsive to immunotherapy (Arino *et al.*, 2016; Gadoth *et al.*, 2017).

Anti-LGI1 associated limbic encephalitis (or anti-LGI1 encephalitis) has an estimated incidence of 0.83 per 1 million persons (van Sonderen *et al.*, 2016), strongly associates with DRB1*07:01-DQB1*02:02 and HLA-DRB4 (Kim *et al.*, 2017; van Sonderen *et al.*, 2017b), and rarely presents as a paraneoplastic manifestation of an underlying thymoma (van Sonderen *et al.*, 2017a). Different from the other autoantigens of limbic encephalitis, which are synaptic receptors or cell membrane proteins, LGI1 is a secreted neuronal protein that has several binding partners, possibly organizing a trans-synaptic complex that includes the pre-synaptic ADAM23 and Kv1.1 potassium channels, and the postsynaptic ADAM22 and AMPAR (Sirerol-Piquer *et al.*, 2006; Fukata *et al.*, 2010). Mutations of LGI1 are linked to a disorder named “autosomal dominant lateral temporal lobe epilepsy” (ADTLE), an inherited form of epilepsy characterized by partial seizures with acoustic or visual hallucinations (Poza *et al.*, 1999; Morante-Redolat *et al.*, 2002; Staub *et al.*, 2002). Several transgenic mouse models expressing a truncated LGI1 mutant that causes the inherited human disease, as well as LGI1 knock-out mice, showed an increase of excitatory synaptic transmission as

compared with wild-type mice (Zhou *et al.*, 2009; Boillot *et al.*, 2016; Seagar *et al.*, 2017). These findings and evidence from experiments in oocytes after overexpression of Kv1.1, Kvbeta1, LGI1, and mutated LGI (Schulte *et al.*, 2006) suggested that LGI1 decreases presynaptic release probability by upregulating presynaptic Kv1 channel activity *in vivo*. On the other hand, LGI1 knock-out mice also had decreased levels of post-synaptic AMPAR in the hippocampal dentate gyrus (Ohkawa *et al.*, 2013).

A previous study examining the synaptic effects of patients' LGI1 antibodies showed that they disrupted the interaction of LGI1 with ADAM22 and reversibly reduced the postsynaptic clusters of AMPAR *in vitro* in rat hippocampal neurons (Ohkawa *et al.*, 2013). The antibodies also altered the interaction of LGI1 with a soluble construct of ADAM23 (Ohkawa *et al.*, 2013) but the effects on Kv1.1 potassium channels and plasticity, the effects in an animal model, and whether patients' antibodies can impair memory were not reported. Considering the interaction of LGI1 with ADAM23, we reasoned that patients' antibodies would have a downstream effect on the Kv1.1 potassium channels. Moreover, since anti-LGI1 encephalitis usually results in a treatable hippocampal syndrome with difficulty in forming new memories (Arino *et al.*, 2016; van Sonderen *et al.*, 2016), we postulated that patients' antibodies would alter memory in a mouse model of cerebroventricular transfer of the antibodies. Our findings reveal a complex pathogenic mechanism of LGI1 antibodies involving both the Kv1.1 potassium channels and AMPAR, which lead to alterations of plasticity and to prolonged but reversible memory deficits.

Material and Methods

Patients´ serum samples

Serum samples of 25 patients with anti-LGI1 encephalitis were included in the assays (Supplementary Table 1). In all cases the presence of LGI1 antibodies was confirmed with rat brain tissue immunohistochemistry and a cell-based assay with human embryonic kidney (HEK)293 cells expressing LGI1 (Lai *et al.*, 2010). Serum samples from 20 antibody-negative healthy blood donors were used as controls. In a subset of experiments (field potential recordings) we additionally used CSF from patients and controls. Studies were approved by the institutional review board of Hospital Clínic and Institut d'Investigacions Biomèdiques August Pi i Sunyer (IDIBAPS), University of Barcelona and Jena University Hospital.

Serum IgG purification

Sera from 8 high-titer LGI1 antibody positive patients with prominent limbic encephalitis were pooled and the IgG (LGI1 IgG) isolated using agarose beads columns (#20423, Pierce), as reported (Gresa-Arribas *et al.*, 2016). IgG similarly isolated from serum of antibody-negative healthy blood donors was used as control (control IgG). After IgG isolation, samples were dialyzed, normalized to a concentration of 4µg/µl using Amicon Ultracentrifugal filters 30K (#UFC903024, Sigma-Aldrich), filtered, and kept at -80 C° until use. The LGI1 specificity of the sample preparation was determined by immunoabsorption with HEK293 cells expressing LGI1, which showed abrogation of reactivity with brain, LGI1-expressing HEK293 cells, and cultured neurons (Supplementary Fig. 1), and by immunohistochemistry with brain of LGI1 null mice which showed lack of immunostaining (Supplementary Fig. 2).

Production of soluble LGI1

HEK293 cells were transfected with a human LGI1 plasmid (Origene, human sequence sc-116925) as reported (Lai *et al.*, 2010). Six hours after transfection, culture medium was replaced with OptiMem medium (#51985-026, Gibco) and cells were

incubated for 15 hours at 37ºC, 95% O_2, 5% CO_2. The medium was then collected and concentrated (total protein, 3 mg/ml) using Amicon Ultracentrifugal filters 30K (#UFC903024, Millipore). The LGI1 enriched medium was then filtered through 0.22µm polyvinylidenedifluoride (PVDF) membrane filters (#sc-358812, Santa Cruz), and the presence of LGI1 in the media was determined by immunoblot using a commercial LGI1 antibody (1:200, #ab30868, Abcam), as described in Supplementary material. The same steps were carried out for the media of non-transfected HEK293 cells (used as control).

LGI1 deletion mutants

To identify the main epitope regions of LGI1, human full length LGI1 DNA, (SC116925; NM_005097, Origene) cloned in pCMV6-AC-GFP plasmid was used as template to generate deletion mutants. The cloning procedures were performed by GenScript (USA, Inc, Piscataway, NJ, USA). Clone #1 corresponded to the indicated human full length LGI1 DNA; clone #2 contained the signal peptide (1-34 nucleotides) and the leucine rich repeat (LRR) domain (35-223 nucleotides); clone #3 contained the signal peptide and the epitempin (EPTP) domains (224-557 nucleotides), and clone #4 had the signal peptide (SP) and the immunoglobulin domain 3 of IgLON5 (218-307 nucleotides of IgLON5) (Sabater *et al.*, 2016) and served as control. In order to anchor the constructs to the cell membrane, all four clones had the glycosylphosphatidylinositol (GPI) sequence and the green fluorescence protein (GFP) sequence of human IgLON5 (RG225495; NM_001101372, Origene) added to the C-terminus. The presence of patients' serum antibodies against each of these clones was determined with a conventional HEK293 cell-based assay, using serum dilutions 1:20 for 1 hour at room temperature, and a secondary goat anti-human IgG Alexa Fluor 594 (1:1000, A11014, Invitrogen) for 1 hour.

LGI1 binding assay

HEK293 cells were transfected with ADAM22 or ADAM23 (rat sequences containing an HA tag) as reported (Lai *et al.*, 2010), and their expression was confirmed with a mouse polyclonal antibody against HA 6E2 (1:200, #2367, Cell Signaling). To show that soluble LGI1 was able to bind to ADAM22 or ADAM23, HEK293 cells expressing ADAM22 or ADAM23 were exposed to the indicated LGI1 enriched medium (1:3) in Dulbecco's Modified Eagle's medium (DMEM) for 2 hours at 37ºC, washed with DMEM, and sequentially incubated for 45 minutes at 37ºC with patients' LGI1 IgG or control IgG (1:50) and goat anti-human IgG Alexa Fluor 488 (1:1000, #A11013, Invitrogen). A similar experiment was performed using goat polyclonal antibody against LGI1 (diluted 1:100, #sc9583, Santa Cruz) instead of human LGI1 IgG; in this setting the secondary antibody was donkey anti-goat Alexa Fluor 488 (1:1000, #A11055, Invitrogen).

Parallel studies in which the indicated medium with soluble LGI1 had been pre-incubated with excess patients' or control IgG (total IgG concentration 0.5 mg/ml) for 2 hours at 37ºC, were used to determine whether patient's antibodies interfered with the binding of soluble LGI1 to cells expressing ADAM22 or ADAM23.

Mice, placement of osmotic pumps, and behavioral tasks

Male C57BL6/J mice (Charles River), 8-10 weeks old (25-30 g) were used in the studies. Animal experiments were performed in accordance to the ARRIVE guidelines for reporting animal research (Kilkenny, Browne, Cuthill, Emerson, & Altman, 2010) and the procedures were approved by the local ethics committee at the Universities of Barcelona and Jena. Detailed information on the animal studies including surgery, placement of ventricular catheters and osmotic pumps, and behavioral tests is provided as supplemental information and has been previously reported (Planaguma *et al.*, 2015).

The distribution of behavioral tests in relation to the infusion of LGI1 IgG control IgG is shown in Supplementary Fig. 3. Overall, a total of 118 mice were used for these studies: 83 for behavioral and brain tissue studies (quantification of Kv1.1 and AMPAR clusters; antibody extraction; immunoprecipitation) and 35 for electrophysiological studies.

Immunofluorescence and confocal microscopy with brain tissue

Representative groups of mice were deeply anesthetized with isoflurane, perfused with PBS, and sacrificed at different time points (days 1, 5, 13, 18, 26, 47). The brains were removed and sagittally split into the two hemispheres. One hemisphere was fixed with 4% PFA for 1 hour, cryopreserved in 40% sucrose for 48 hours, embedded in optimal cutting temperature compound (#4583, Tissue-Tek), and snap frozen in isopentane chilled with liquid nitrogen.

To determine the levels of presynaptic Kv1.1 potassium channels, 5 μm thick cryostat sections were sequentially incubated with a polyclonal rabbit antibody against Kv1.1 (1:100, #ab32433, Abcam) for 2 hours at RT, washed in PBS containing 0,3% Triton, and incubated with a mouse monoclonal antibody against the presynaptic marker Bassoon (1:250, #SAP7F407, Enzo), overnight at 4°C. Secondary antibodies included goat anti-rabbit Alexa Fluor 488 and goat anti-mouse Alexa Fluor 594 (both 1:1000, #A11008 and A11005, Invitrogen).

To determine whether the post-synaptic levels of AMPAR were affected, brain sections were incubated with a polyclonal guinea pig antibody against GluA1 (1:200, #AGP009, Alomone) for 2 hours at RT, washed in PBS containing 0,3% Triton, and incubated with a rabbit polyclonal antibody against the post-synaptic marker PSD95 (1:250, #18258, Abcam) overnight at 4°C. Secondary antibodies included goat anti-guinea pig Alexa Fluor 488, and goat anti-rabbit Alexa Fluor 594 (1:1000, #A11073 and

A11012, Invitrogen). The AMPAR that co-localized with PSD95 were defined as synaptic.

Cell-surface and synaptic clusters of the indicated proteins were visualized and quantified by confocal imaging (LSM710, Carl-Zeiss, Germany) using Imaris suite 7.6.4 (Bitplane AG, Zürich, Switzerland), as reported (Planaguma *et al.*, 2015).

Acid-extraction of human antibodies from hippocampal tissue

The contralateral hippocampus was dissected under a magnifying glass (Zeiss stereomicroscope, Stemi 2000), washed with cold PBS, homogenized in PBS containing a cocktail of protease inhibitors (1:50, #P8340, Sigma-Aldrich), and centrifuged at 16000 rpm for 5 minutes. The supernatant was separated and kept as pre-extraction fraction; the pellet was resuspended in 0.1M Na-citrate buffer pH 2.7 for 15 minutes on ice, centrifuged (16000 rpm, 5 minutes), and the supernatant containing the acid-extracted human IgG was separated and neutralized with 1.5 M Tris buffer pH8.8 (extraction fraction). The presence of human LGI1 antibodies in the pre-extraction and extraction fractions was assessed with the indicated HEK293-LGI1 cell-based assay (Lai *et al.*, 2010).

LGI1 immunoprecipitation from brain tissue

Representative mice brain from animals infused for 14 days with LGI1 IgG or control IgG were used for this experiment. Brains were removed, washed with PBS, and homogenized with cold lysis buffer (NaCl 150 mM, EDTA 1 mM, Tris-HCl 100mM, Deoxycholic acid 0.5%, Triton X-100 1%) and a cocktail of protease inhibitors (1:50, #P8340, Sigma). After centrifugation (16000 rpm for 20 minutes), the supernatant was retained and the IgG contained in the supernatant was isolated with protein A/G agarose beads (#20424, Thermo Fisher). The precipitated beads containing IgG were then run in a 4-12% BisTris electrophoresis gel (#NP03222 NuPage, Invitrogene), transferred into a

nitrocellulose membrane (#1704158, Biorad), probed with a commercial antibody against LGI1 (1:200, #ab30868, Abcam), and the reactivity developed with a peroxidase-linked secondary antibody (Anti-rabbit 1:1000, #NA934V, GE HealthCare) using the chemiluminiscence method and read with an ImageQuant LAS 4000 Control Software (GE Healthcare).

Electrophysiological Recordings

Preparation of acute hippocampal brain slices was done 14-16 days after pump implantation. Mice were deeply anesthetized, decapitated, and the brain was removed in ice-cold protective cutting artificial cerebrospinal fluid (aCSF1 for patch-clamp recordings (in mM); 95 N-Methyl-D-glutamine, 30 $NaHCO_3$, 20 HEPES, 25 glucose, 2.5 KCl, 1.25 NaH_2PO_4, 2 thiourea, 5 sodium ascorbate, 3 sodium pyruvate, 10 $MgSO_4$, 0.5 $CaCl_2$, 12 N-acetylcysteine, adjusted to pH 7.3 and an osmolarity of 300 to 310 mOsmol, purged with 95% O_2/5% CO_2)(Grunewald *et al.*, 2017) or in high-sucrose extracellular artificial fluid (aCSF2 for field potential recordings (in mM); 206 sucrose, 1.3 KCl, 1 $CaCl_2$, 10 $MgSO_4$, 26 $NaHCO_3$, 11 glucose, 1.25 NaH_2PO_4; purged with 95% CO_2/5% O_2, pH 7.4). The brain was then subdivided into the hemispheres and coronal hippocampal slices (300 µm for patch-clamp recordings and 380 µm for field potential recordings) were prepared on a vibratome (Leica, Wetzlar, Germany; Leica VT1200 S).

Whole-cell patch-clamp recordings of dentate gyrus granule cells

Slices were then incubated in aCSF1 at 34°C for 12 minutes and transferred into another incubation beaker with protective storage aCSF3 (in mM: 125 NaCl, 25 $NaHCO_3$, 25 glucose, 2.5 KCl, 1.25 NaH_2PO_4, 1 $MgCl_2$, 2 $CaCl_2$, 2 thiourea, 5 sodium ascorbate, 3 sodium pyruvate, 12 N-acetylcysteine, adjusted to pH 7.3 and an

osmolarity of 300 to 310 mOsmol, purged with 95% O_2/5% CO_2) at RT for at least 1 hour until recording.

Electrophysiological measurements were performed with a HEKA EPC-10 double patch-clamp amplifier with a sampling rate of 20 kHz. All recordings were filtered at 2.9 and 10 kHz using Bessel filters of the amplifier. For whole-cell patch-clamp recordings single slices were transferred into a recording chamber and continuously submerged with recording aCSF4 (in mM: 125 NaCl, 25 $NaHCO_3$, 25 Glucose, 2.5 KCl, 1.25 NaH_2PO_4, 1 $MgCl_2$, 2 $CaCl_2$, purged with 95% O_2/5% CO_2) at RT (Haselmann *et al.*, 2015). Measurements were done on dentate gyrus granule cells of the hippocampus at holding potentials of -70 mV. Patch pipettes were pulled from thick-walled borosilicate glass and filled with intracellular solution (in mM:120 K-gluconate, 20 KCl, 10 HEPES, 0.1 EGTA, 4 Mg-ATP, 0.2 Na_2-GTP, 2 $MgCl_2$, 10 Na-Phosphocreatine, adjusted to pH 7.3 with CsOH and an osmolarity of 280 mOsmol) and had a final resistance of 2.5 – 5 MΩ. Series resistance was compensated (70-80%) and monitored during the recordings. For evaluation of evoked excitatory postsynaptic currents (eEPSCs) the medial perforant path (MPP) was stimulated by a theta glass bipolar electrode filled with aCSF4 and connected to a stimulus isolation unit (Isoflex, A.M.P.I, Jerusalem, Israel). Supramaximal stimulation was determined when increasing stimulation did not result in an increase of eEPSC and ranged from 200 – 400 µA. For isolation of AMPAR-mediated glutamatergic transmission, 50 µM 2-amino-5-phosphonovalerate (AP-5, #0106,Tocris) and 20 µM bicuculline (#0109, Tocris) in aCSF4 perfusion were used to block NMDA receptor and GABAa receptor, respectively. Paired-pulse facilitation of eEPSC was measured with interstimulus intervals of 50 ms after supramaximal stimulation. Whole cell recordings were analyzed by NeuroMatic plugin of Igor Pro Software 6 or 7 (Wavemetrics, Portland, OR, USA).

Cells with series resistance >30MΩ or series resistance changes of >20% during measurement were discarded. Liquid junction potential of 10 mV was corrected offline for all whole-cell patch clamp recordings.

Field potential recordings and analysis of long-term potentiation (LTP)

380 µm thick coronal hippocampal slices were transferred into an incubation beaker with aCSF5 (in mM: 119 NaCl, 2.5 KCl, 2.5 $CaCl_2$, 1.25 NaH_2PO_4, 1.5 $MgSO_4$, 25 $NaHCO_3$, 11 glucose, purged with 95 % CO_2/5 % O_2 pH 7.4). Slices were kept at 32°C for 60 minutes and subsequently at RT for at least 60 additional minutes. Slices were then transferred into a measurement chamber perfused with aCSF5 at 32°C. A bipolar stimulation electrode (Platinum-Iridium stereotrode, Science Products) was placed in the Schaffer collateral pathway (Planaguma *et al.*, 2016). Recording electrodes were made from borosilicate glass (BF150-86-10, Sutter Instruments). The recording electrode filled with aCSF5 was placed in the dendritic branching of the CA1 region for local field potential measurement (field excitatory postsynaptic potential, fEPSP). Signals were amplified and stored using AxoClamp 2B amplifier (Molecular Devices). A stimulus isolation unit A385 (World Precision Instruments) was used to elicit stimulation currents. Before baseline recordings, input-output curves were determined for each slice with stimulation currents ranging from 25 to 700 µA at 0.03 Hz. The stimulation current was adjusted for each recording to evoke fEPSP which was at half of its maximal evoked amplitude. After baseline recordings for 30 minutes with 0.03 Hz, LTP was induced by theta-burst stimulation (TBS; 10 theta bursts of 4 pulses of 100 Hz with an interstimulus interval of 200ms, repeated 7 times with 0.03 Hz). After LTP induction, fEPSPs were recorded for additional 60 minutes with 0.03 Hz. Recordings with unstable baseline measurements (variations higher than 20% in baseline fEPSPs) were discarded.

The recordings were done and analyzed using Axon pCLAMP Software (Molecular Devices, version 10.6). Slopes of all recordings were measured within 1-1.5ms of the linear part of the rising fEPSP before it reaches the peak and starting after the fiber volley. For determination of TBS induced LTP, mean slope values of fEPSPs after TBS until end of the recording were compared between the experimental groups.

Golgi–Cox staining, Sholl analysis, and synaptic spine quantification

Morphological dendrite and spine analysis were performed in granule cells of the dentate gyrus and pyramidal neurons of the CA1 region from the contralateral brain hemisphere of mice used in neurophysiological recordings. Directly after removal, Golgi silver impregnation was conducted with the FD Rapid GolgiStainTM Kit (FD NeuroTechnologies, Inc., Columbia, USA) according to manufacturer's instructions. Dendritic complexity was assessed with the Sholl ring method, including analysis of total dendritic length, number of branch ends, and number of dendrites per branch order. Density of dendritic spines was analyzed in tertiary branches of CA1 pyramidal neurons. Spines were subclassified (thin, mushroom, stubby, filopodia or branched) according to previous reports (McKinney, 2010). Detailed information on Golgi-Cox staining Sholl and dendritic spine analysis is provided as supplemental information.

Statistical analysis

Confocal cluster densities of GluA1, Kv1.1, PSD95, or Bassoon, and behavioral tests with multiple time points (NOR, LOC, RI, ANH) were analyzed using two-way analysis of variance (ANOVA). All behavioral paradigms with single time points (BW, EPM) were analyzed with independent sample *t*-tests; *Post-hoc* analyses for all experiments used Bonferroni correction for multiple testing.

Electrophysiological measurements of In-Out curves were analyzed with two-way ANOVA followed by Holm-Sidak *post-hoc* test. Group comparisons of independent

recordings were made using two-tailed *t*-tests. The alpha-level used to determine significance was $P < 0.05$. All tests were done using GraphPad Prism (Version 7) or SigmaPlot (Version 13.0).

Results

Patients' LGI1 IgG preferentially prevents the binding of LGI1 to ADAM23 as compared to ADAM22

To determine whether patients' LGI1 IgG recognized soluble LGI1 and prevented its binding to ADAM22 or ADAM23, HEK293 cells expressing each of these proteins were incubated with LGI1-enriched or control media. The presence of LGI1 in the media was first confirmed with immunoblot (Fig. 1A, lane 1), and the binding of soluble LGI1 to ADAM22 or ADAM23 was demonstrated in HEK293 cells expressing each of these proteins incubated with soluble LGI1 followed by patients' LGI1 IgG (Fig. 1B) or a commercial LGI1 antibody (data not shown). Pre-incubation of soluble LGI1 with excess patients' LGI1 IgG, but not control IgG, abrogated the binding of LGI1 to ADAM23 (25 of 25 cases [100%]) more consistently than to ADAM22 (15/25 [60%]) (Fig. 1B, and Supplementary Fig. 4).

The target epitopes of LGI1 IgG are more frequently located in the LRR than in the EPTP domains

All patients' samples strongly reacted with clones 1 and 2 which contained the LRR domain; 12/25 samples mildly reacted with clone 3 which contained the EPTP domain, and none with clone 4 which contained the signal peptide (SP) domain of LGI1 sequence followed by the immunoglobulin domain 3 of IgLON5 (Fig. 2). None of 20 control sera showed reactivity with any of the four clones (data not shown). These

findings indicate that patients' IgG is directed against epitopes located in the LRR and flanking regions, and less frequently in the EPTP domains.

Passive transfer of patients' LGI1 IgG causes memory deficits in mice

Compared with animals infused with control IgG, those infused with patients' LGI1 IgG showed a progressive decrease of the object recognition index, indicative of a memory deficit (Bura *et al* 2007; Taglialatela *et al*. 2009; Puighermanal *et al*. 2009). The memory deficit became significant on day 3 and persisted until day 25 (11 days after the infusion of IgG had stopped). At the last time point (day 47), the object recognition index had normalized and was similar to that of animals treated with control IgG (Fig. 3). For all time-points, the total time spent exploring both objects (internal control) was similar in animals infused with control or patients' LGI1 IgG (data not shown).

No significant differences were noted in tests of anxiety (black and white test, elevated plus maze test), aggression (resident-intruder test) and locomotor activity (Supplementary Fig. 5).

Passive transfer of patients' LGI1 IgG causes a decrease of Kv1.1 potassium channels and AMPAR

The presence of patients' IgG bound to LGI1 in mice brain tissue was demonstrated with two techniques: immunoprecipitation of LGI1 using protein A/G agarose beads (Supplementary Fig. 6A), and acid-extraction of human antibodies from hippocampus that reacted with LGI1 expressed in HEK293 cells (Supplementary Fig. 6B). To determine whether patients' LGI1 IgG had effects on Kv1.1 and AMPAR clusters we focused on the hippocampus (Fig. 4A). This region was selected because anti-LGI1 encephalitis predominantly affects the hippocampus which has close proximity to the lateral ventricles where the IgG fractions were infused. Compared with animals infused

with control IgG those infused with patients' LGI1 IgG had on days 13, 18, and 26 a significant decrease of the density of cell surface and synaptic Kv1.1 clusters (Fig. 4B-D) followed by a gradual recovery after day 26 (pooled analysis of the subregions in CA1, CA3, and dentate gyrus [DG] indicated in Fig. 4A). In contrast, patients' LGI1 IgG did not affect the density of the presynaptic marker Bassoon (Fig. 4E).

In parallel we investigated whether the levels of cell surface and synaptic AMPAR (GluA1) clusters were affected in the same hippocampal subregions used for the Kv1.1 studies. The findings showed that mice infused with patients' LGI1 IgG had on day 18 a significant decrease of cell surface and synaptic AMPAR compared with mice infused with control IgG (Fig. 5A-C). The total cell surface AMPAR appeared to decrease and recover faster than the synaptic AMPAR. No significant differences were noted in the levels of PSD95 clusters comparing mice infused with patients' or control IgG (Fig. 5D).

Patients' LGI1 IgG increases excitatory synaptic transmission

To investigate the pathophysiological role of patients' LGI1 IgG in synaptic transmission, we examined the glutamatergic transmission by whole-cell patch-clamp recordings in acute brain slices of mice after the indicated 14-day cerebroventricular infusion of patients' LGI1 IgG or control IgG. LGI1 is predominantly expressed in the hippocampal formation where it colocalizes with Kv1.1 in the middle molecular layer of the dentate gyrus (Schulte et al., 2006). We therefore recorded electrically evoked (e)EPSCs in the DG granule cells (GC) of the hippocampus. We did not observe any differences in membrane properties, e.g. series resistance, resting membrane potential, or cell capacitance in both groups (not shown). Incremental stimulation of axons in the MPP from the entorhinal cortex led to increased peak amplitudes of eEPSCs in slices of mice infused with patients' LGI1 IgG as compared to control IgG, whereas eEPSC

kinetics remained unchanged (Fig. 6A-D). This increase of excitatory synaptic transmission could either result from altered AMPAR formation on the postsynaptic density or from an increased presynaptic release of glutamate. To determine whether short-term plasticity was altered in patients' LGI1 IgG treated mice, we performed paired-pulse recordings in the MPP-GC pathway. Mice infused with patients' LGI1 IgG showed reduced paired-pulse facilitation as compared to control IgG infused mice (Fig. 6E, F). Together, these data suggest that mice with chronic infusion of LGI1-IgG have alterations in presynaptic function characterized by increased neurotransmitter release.

Patients' LGI1 IgG alters synaptic plasticity

Next, we examined synaptic plasticity in the hippocampus by recording field potentials (fEPSPs) in the CA1 pathway after stimulation of the Schaffer collateral in hippocampal slices of mice infused with patients' LGI1 IgG and control IgG. The findings showed impaired LTP in slices of mice infused with patients' LGI1 IgG as shown by reduced fEPSP slope values throughout the recording period up to 60 minutes after theta-burst stimulation (Fig. 7A-C).

Dendritic pruning is unaffected by patient´s LGI1 IgG

In a previous report using a transgenic mouse model with a truncated form of LGI1, abnormal dendritic pruning and increased spine density was associated with increased excitatory synaptic transmission (Zhou *et al.*, 2009). Here, we investigated dendritic pruning and spine morphology in mice infused with patients' LGI1 IgG and control IgG. Sholl analysis with concentric shells and neurolucida reconstructions of dentate gyrus granule cells showed unchanged dendritic arborization and dendrite length after infusion of patients' LGI1 IgG (Fig. 8A-E). Analysis of synaptic spines in CA1 apical dendrites revealed identical spine density and unchanged spine morphology in both

experimental groups (Fig. 8F-H). Thus, changes in excitatory transmission and synaptic plasticity were not mediated by defective synaptic maturation.

Discussion

We show that patients' LGI1 antibodies alter the levels of Kv1.1 potassium channels and AMPAR causing a severe impairment of memory, plasticity, and neuronal transmission in a passive transfer mouse model of patient-derived antibodies. Previous clinical reports demonstrated that despite the severity of anterograde memory deficits most patients improved with immunotherapy (Arino *et al.*, 2016; van Sonderen *et al.*, 2016; Gadoth *et al.*, 2017), and experimental studies provided evidence that patients' antibodies caused a decrease of AMPAR in cultured neurons (Ohkawa *et al.*, 2013). Together, these findings suggested the pathogenicity of LGI1 autoantibodies but the effects on an animal model were pending to investigate. Here we used a model of cerebroventricular transfer of patients´ antibodies to mice because the proximity of the lateral ventricles to the hippocampus facilitates exploring the alterations on memory and plasticity. It is likely that defective plasticity in the hippocampus of mice treated with patients' LGI1 IgG may underlie the observed memory deficit and that similar mechanisms apply to the short-term memory deficit of the patients.

LGI1 is a neuronal secreted protein containing an N-terminal LRR-domain and a C-terminal EPTP domain (Fukata *et al.*, 2006; Sirerol-Piquer *et al.*, 2006). Previous studies have shown that LGI1 interacts with the transmembrane metalloproteases ADAM23 and ADAM22 (Fukata *et al.*, 2006) that serve as receptors associated with presynaptic and axonal complexes containing Kv1.1 channels and postsynaptic AMPAR, respectively. Using IgG fractions of 25 patients with anti-LGI1 encephalitis we found that all patients´ IgG strongly reacted with the LRR domain of LGI1 and only

12 of 25 samples showed reactivity with the EPTP domain, thus suggesting that the LGI1 LRR domain contains dominant epitopes of LGI1 antibodies. Since the EPTP domain is essential for binding of LGI1 to ADAM22 (Fukata *et al.*, 2006), we hypothesize that pathogenic antibodies more frequently affect the interaction of LGI1 with presynaptic ADAM23. Nevertheless, we and others have observed that 60% of the patients harbor antibodies that also inhibit the interaction of LGI1 with ADAM22 (Ohkawa *et al.*, 2013).

Mice with mutated or deficient LGI1 show a severe epileptic phenotype with premature death (Zhou *et al.*, 2009; Chabrol *et al.*, 2010; Fukata *et al.*, 2010; Yu *et al.*, 2010). In these models, two potential underlying mechanisms have been reported including, loss of synaptic AMPAR leading to reduction of AMPAR-mediated glutamatergic transmission (Fukata *et al.*, 2010; Lovero *et al.*, 2015), and defective function of axonal and presynaptic Kv1.1 resulting in enhanced excitatory transmission (Yu *et al.*, 2010; Boillot *et al.*, 2016; Seagar *et al.*, 2017). Here, after continuous intraventricular infusion of patients´ LGI1 IgG, we found significant reduction of AMPAR and Kv1.1 clusters in the hippocampus, corroborating previous observations in LGI1 knockout mouse models (Fukata *et al.*, 2010; Lovero *et al.*, 2015; Seagar *et al.*, 2017). Moreover, in acute sections of hippocampus of mice infused with LGI1 IgG, but not in those infused with control IgG, we found distinct functional evidence for hyperexcitability and enlarged glutamatergic transmission in the MPP-GC pathway compatible with increased presynaptic release.

These findings are in agreement with a previous report showing increased firing frequency and enlarged evoked glutamatergic transmission in CA3 neurons after preincubation of brain slices with IgG from patients with limbic encephalitis and antibodies against proteins of the voltage-gated K^+ channel complex (Lalic *et al.*, 2011)

which presumably were directed against LGI1 (Irani *et al.*, 2010; Lai *et al.*, 2010). It is known that presynaptic Kv1.1 potassium channel inactivation enhances release probability by increased and prolonged depolarization, Ca^{2+} influx, and subsequent potentiation of excitatory transmission (Geiger and Jonas, 2000). Indeed, recent studies in slice cultures or acute slices of LGI1 knockout mice showed evidence for enhanced neuronal excitability, increased release of presynaptic glutamate, and enlarged excitatory synaptic drive (Boillot *et al.*, 2016; Seagar *et al.*, 2017). In an oocyte expression system LGI1 has been shown to prevent the N-type inactivation of Kv1.1 channels. Mutated LGI1 reversed this effect, thus leading to rapid inactivation possibly contributing to an increase of action potential broadening and glutamate release (Schulte *et al.*, 2006). Together, in the passive-transfer model of LGI1 IgG we identified several underlying pathophysiological mechanisms that are in good agreement with previous observations in LGI1 deficient model systems. Our findings point toward interference with LGI1 associated pathways that affect LGI1 signaling via post- and presynaptic mechanisms.

In our model of ventricular transfer of antibodies we did not observe seizures, but electrographic recordings were not performed. The mouse strain of our model was selected to determine the LGI1 antibody effects on memory and behavior, but there are mouse strains more appropriate to investigate potential increased seizure susceptibility (Ferraro *et al.*, 2002). At the synaptic level the findings in the LGI1 deficient models as well as in our immune-mediated model make difficult to explain how reduced AMPAR function associates with epileptic seizures in patients with ADTLE or anti-LGI1 encephalitis. Homeostatic downregulation of postsynaptic AMPAR in response to an ongoing presynaptic hyperexcitability has been proposed but it remains speculative and is not yet supported by experimental evidence (Seagar *et al.*, 2017). This hypothesis

however, is in line with the observation that patients' LGI1 IgG caused a reduction of Kv1.1 expression (from day 5 after onset of antibody infusion) that preceded the reduction of AMPAR clusters (from day 13) in the hippocampus of infused mice.

In ADAM23 deficient mice (Owuor *et al.*, 2009) as well as in a transgenic model with truncated LGI1 (Zhou *et al.*, 2009), abnormal maturation of hippocampal synapses was observed. These changes consisted of decreased dendritic arborization in ADAM23 deficient mice but defective synaptic pruning and increased spine density in LGI mutant mice. Different from these observations in germline knockout strains, application of LGI1 antibodies in adult mice did not induce changes in spine density or dendritic arborization. Furthermore, we did not detect any differences in neuronal membrane properties such as cell capacitance or input resistance. This is likely explained by the acute disturbance of LGI1 function by specific autoantibodies in the mature brain in contrast to chronic changes and adaptions in neuronal network following genetic mutation. Corroborating these findings, a recent report revealed unchanged synaptic density and dendritic arborization in very young LGI1 knockout mice before onset of epileptic activity (Boillot *et al.*, 2016).

Overall, intraventricular application of patients' LGI1 IgG caused severe impairment of memory and plasticity along with neuronal hyperexcitability and alterations of the levels of Kv1.1 and AMPAR similar to those reported in models of genetic alteration of LGI1, providing evidence of antibody pathogenicity. Since LGI1 is a neuronal secreted linker protein, the antibody-mediated disturbance of this synaptic complex signaling pathway leads to fundamentally different pathophysiological mechanisms as compared with those associated with other antibody-mediated diseases, such as anti-NMDAR or anti-AMPAR encephalitis, where the antibodies alter the cell surface dynamics of the targets and cause their internalization (Mikasova *et al.*, 2012;

Peng *et al.*, 2015). Interestingly, among the few antibody-mediated encephalitides that more frequently manifest as limbic encephalitis (Dalmau and Graus, 2018), two of them associate with antibodies that cause an important reduction of AMPAR, either by direct binding of the antibodies to the receptor (anti-AMPAR encephalitis) or by binding to synaptic partners, as shown here for LGI1. A task for the future is to clarify how antibody-binding to the protein-protein interaction domains of LGI1 (LRR, EPTP) affects LGI1 conformation and reactivity to its binding partners, and whether different approaches of antibody transfer (parenchymal, cortical) in different strains of mice lead to epileptic activity and seizures.

Acknowledgements

We thank Claudia Sommer (Jena), Esther Aguilar (Barcelona), and Mercè Alba (Barcelona) for providing expert technical assistance in animal experiments.

Funding

This work was supported by the Deutsche Forschungsgemeinschaft (CRC-TR 166 [TP B2 to C.G. GE2519_3-1 to C.G.), by the IZKF and CSCC Jena to C.G.), Instituto Carlos III/FEDER (FIS PI15/00377, FG; FIS PI14/00203, JD, FIS PI14/00141, XG; FIS PI17/00296, XG; RETIC RD16/0008/0014, XG), Fondation de l'Université de Lausanne et Centre Hospitalier Universitaire Vaudois (UNIL/CHUV), Lausanne, Switzerland (MS), NIH (RO1NS077851, JD), Ministerio de Economia, Industria y Competitividad, Spain (BFU2017-83317-P, DS), AGAUR (SGR93, JD; SGR737, XG), CERCA Programme / Generalitat de Catalunya,), (PERIS) (SLT002/16/00346, JP), and Fundació CELLEX (JD). The authors declare no conflict of interest.

Legends to figures

Figure 1: Patient's LGI1 IgG blocks the binding of soluble LGI1 to ADAM22 and ADAM23

The media of HEK293 cells transfected with LGI1 contains secreted LGI1 (A, lane 1) whereas the media of non-transfected cells does not contain LGI1 (A, lane 2). HEK293 cells expressing ADAM22 or ADAM23 bind soluble LGI1 present in the media of HEK293 cells expressing LGI1 (B, first row) but not present in control media (B, second row). When the media with soluble LGI1 is pre-incubated with a representative patient's LGI1 IgG the binding of LGI1 to ADAM22 or ADAM23 is abrogated (B, third row); in contrast, no blocking of the binding is observed when the media is pre-incubated with control IgG (B, fourth row). Scale bar = 20 μm.

Figure 2: Reactivity of a patient's serum with deletion constructs of LGI1

Serum from a representative patient with anti-LGI1 encephalitis shows predominant reactivity with the full-length sequence of LGI1 (clone 1), and the construct that contains the LRR domain (clone 2); milder reactivity is shown with the construct that contains the EPTP domain (clone 3). The construct generated by clone 4 contains the signal peptide (SP) but does not include any LGI1 sequence. Scale bar = 20 μm.

Figure 3: Cerebroventricular infusion of patients' LGI1 IgG causes decrease of memory

Novel object recognition index in mice treated with patients' IgG (red, n = 16) or control IgG (grey, n = 14). A high index indicates better memory. Data is presented as mean ± SEM. *P<0.05; **P<0.01.

Figure 4: Patients' LG1 IgG causes a decrease of total cell surface and synaptic Kv1.1 clusters in the hippocampus

Sagittal section of hippocampus of a representative mouse infused with patients' LGI1 IgG demonstrating the immunostaining of Kv1.1, Bassoon, and the merging reactivities (A). Squares in "Analysis" indicate the analyzed subregions in CA1, CA3, and DG for each animal. Scale bar = 200 µm. 3D projection and analysis of the density of total cell surface clusters of Kv1.1 and Bassoon, and synaptic clusters of Kv1.1 (defined as Kv1.1 clusters that co-localized with Bassoon) in one of the indicated CA3 subregions (A "Analysis"). Merged images (B, left upper and lower squares; Kv1.1 green, and Bassoon red) were post-processed and used to calculate the density of the indicated clusters (density = spots/µm^3). Scale bar = 2 µm. Quantification of the density of total cell surface (C) and synaptic (D) Kv1.1 clusters, and Bassoon clusters (E) in a pooled analysis of hippocampal subregions (CA1, CA3, DG) in animals treated with patients' LGI1 IgG (red) or control IgG (black) on the indicated days. Mean density of clusters in control IgG treated animals was defined as 100%. Data are presented as mean ± SEM. For each time point five animals infused with patients' LGI1 IgG and five with control IgG were examined. Significance of treatment effect was assessed by two-way ANOVA with an alpha-error of 0.05 (asterisks) and *post-hoc* testing with Sidak-Holm adjustment. **P< 0.01; ***P<0.001; ****P<0.0001.

Figure 5: Patients' LG1 IgG causes a decrease of total cell surface and synaptic AMPAR clusters in the hippocampus

3D projection and analysis of the density of total cell surface clusters of GluA1 AMPAR and PSD95, and synaptic clusters of AMPAR (defined as AMPAR clusters that co-localized with PSD95) in one of the CA3 subregions indicated in Fig. 4A, "Analysis". Merged images (A, left upper and lower squares; GluA1 green, and PSD95 red) were post-processed and used to calculate the density of the indicated clusters (density = spots/μm^3). Scale bar = 2 μm. Quantification of the density of total cell surface (B) and synaptic (C) GluA1 AMPAR clusters, and PSD95 clusters (D) in a pooled analysis of hippocampal subregions (CA1, CA3, DG) in animals treated with patients' LGI1 IgG (red) or control IgG (black) on the indicated days. Mean density of clusters in control IgG treated animals was defined as 100%. Data are presented as mean ± SEM. For each time point five animals infused with patients' IgG and five with control IgG were examined. Significance of treatment effect was assessed by two-way ANOVA with an alpha-error of 0.05 (asterisks) and *post-hoc* testing with Sidak-Holm adjustment. **P*< 0.05; ***P*< 0.01; ****P*<0.001; *****P*<0.0001.

Figure 6: Patients'LGI1 IgG increases excitatory synaptic transmission

Evoked excitatory postsynaptic currents (eEPSCs) in dentate gyrus granule cells upon incremental stimulation of medial perforant path (MPP) afferent fibers are increased in acute brain slices of mice that received patient´s LGI1 IgG (A and B). Example traces of an individual recording are shown in (A). In/out characteristics of granule cell neurons of control IgG and patients' LGI1 IgG treated mice (B; $n_{control\ IgG}$ = 13; $n_{LGI1\ IgG}$ = 15; data are presented as mean ± SEM; two-way ANOVA and Holm-Sidak *post-hoc* test. ****P*<0.001). Peak amplitude of eEPSCs (example traces in C) is increased after

infusion of antibodies against LGI1, whereas rise and decay time is unchanged ($n_{control\ IgG}$ = 13; $n_{LGI1\ IgG}$ = 15; data are presented as mean ± SEM; unpaired *t*-test. ***P*<0.01) (C and D). Paired pulse facilitation with an interstimulus interval of 50 ms is reduced in granule cell neurons from mice after infusion of patients' LGI1 IgG indicating increased release probability. Example traces in E; dashed lines indicate peak amplitude of the first pulse ($n_{control\ IgG}$ = 11; $n_{LGI1\ IgG}$ = 13; data are presented as mean ± SEM; unpaired *t*-test. **P*<0.05) (E and F).

Figure 7: Patients' LGI1 IgG alters synaptic plasticity

Example traces of individual field excitatory postsynaptic potential (fEPSP) recordings in the CA1 region before and after theta burst stimulation (TBS) of Schaffer collateral afferents show reduced fEPSP potentiation in brain slices of mice that received patient´s LGI1 IgG (A). Time course and quantitative analysis of long-term potentiation (LTP) after TBS (arrow), demonstrates persistent reduction of fEPSP slope values in slices of mice after infusion of patient´s LGI1 IgG indicating disturbed synaptic plasticity. Quantification of fEPSP slope change is decreased in LGI1 IgG infused mice (B and C, $n_{control\ IgG}$ = 10; $n_{LGI1\ IgG}$ = 13; data are presented as mean ± SEM; unpaired *t*-test. **P*<0.05).

Figure 8: Dendritic pruning is unaffected by patients' LGI1 IgG

Dendritic arborization of a dentate gyrus granule cell; example neuron is shown after Golgi silver impregnation (left) and in Neurolucida reconstruction for Sholl analysis (right) (A, scale bar = 50 µm). Sholl analysis revealed unchanged dendritic arborization in control IgG and patients' LGI1 IgG infused mice as shown by the length of hippocampal granule cell dendrites (B and C) and by number and intersection of

dendritic branches (D and E). Synaptic spines of tertiary dendrites of CA1 pyramidal neurons (F, scale bar = 10μm). Quantification of spine density (G) and of spine morphology (H) is unchanged in control IgG and patients' LGI1 IgG infused mice (all data are presented as mean ± SEM).

References

Arino H, Armangue T, Petit-Pedrol M, Sabater L, Martinez-Hernandez E, Hara M*, et al.* Anti-LGI1-associated cognitive impairment: Presentation and long-term outcome. Neurology 2016; 87(8): 759-65.

Boillot M, Lee CY, Allene C, Leguern E, Baulac S, Rouach N. LGI1 acts presynaptically to regulate excitatory synaptic transmission during early postnatal development. Sci Rep 2016; 6: 21769.

Chabrol E, Navarro V, Provenzano G, Cohen I, Dinocourt C, Rivaud-Pechoux S*, et al.* Electroclinical characterization of epileptic seizures in leucine-rich, glioma-inactivated 1-deficient mice. Brain 2010; 133(9): 2749-62.

Dalmau J, Geis C, Graus F. Autoantibodies to Synaptic Receptors and Neuronal Cell Surface Proteins in Autoimmune Diseases of the Central Nervous System. Physiol Rev 2017; 97(2): 839-87.

Dalmau J, Graus F. Antibody-Mediated Encephalitis. N Engl J Med 2018; 378(9): 840-51.

Ferraro TN, Golden GT, Smith GG, DeMuth D, Buono RJ, Berrettini WH. Mouse strain variation in maximal electroshock seizure threshold. Brain Res 2002; 936(1-2): 82-6.

Fukata Y, Adesnik H, Iwanaga T, Bredt DS, Nicoll RA, Fukata M. Epilepsy-related ligand/receptor complex LGI1 and ADAM22 regulate synaptic transmission. Science 2006; 313(5794): 1792-5.

Fukata Y, Lovero KL, Iwanaga T, Watanabe A, Yokoi N, Tabuchi K*, et al.* Disruption of LGI1-linked synaptic complex causes abnormal synaptic transmission and epilepsy. Proc Natl Acad Sci USA 2010; 107(8): 3799-804.

Gadoth A, Pittock SJ, Dubey D, McKeon A, Britton JW, Schmeling JE*, et al.* Expanded phenotypes and outcomes among 256 LGI1/CASPR2-IgG-positive patients. Ann Neurol 2017; 82(1): 79-92.

Geiger JR, Jonas P. Dynamic control of presynaptic Ca(2+) inflow by fast-inactivating K(+) channels in hippocampal mossy fiber boutons. Neuron 2000; 28(3): 927-39.

Gresa-Arribas N, Planaguma J, Petit-Pedrol M, Kawachi I, katada S, Glaser CA*, et al.* Human neurexin-3alpha antibodies associate with encephalitis and alter synapse development. Neurology 2016; 86(24): 2235-42.

Grunewald B, Lange MD, Werner C, O'Leary A, Weishaupt A, Popp S*, et al.* Defective synaptic transmission causes disease signs in a mouse model of juvenile neuronal ceroid lipofuscinosis. Elife 2017; 6.

Haselmann H, Ropke L, Werner C, Kunze A, Geis C. Interactions of Human Autoantibodies with Hippocampal GABAergic Synaptic Transmission - Analyzing Antibody-Induced Effects ex vivo. Front Neurol 2015; 6: 136.

Irani SR, Alexander S, Waters P, Kleopa KA, Pettingill P, Zuliani L*, et al.* Antibodies to Kv1 potassium channel-complex proteins leucine-rich, glioma inactivated 1 protein and contactin-associated protein-2 in limbic encephalitis, Morvan's syndrome and acquired neuromyotonia. Brain 2010; 133(9): 2734-48.

Irani SR, Stagg CJ, Schott JM, Rosenthal CR, Schneider SA, Pettingill P*, et al.* Faciobrachial dystonic seizures: the influence of immunotherapy on seizure control and prevention of cognitive impairment in a broadening phenotype. Brain 2013; 136(Pt 10): 3151-62.

Kim TJ, Lee ST, Moon J, Sunwoo JS, Byun JI, Lim JA*, et al.* Anti-LGI1 encephalitis is associated with unique HLA subtypes. Ann Neurol 2017; 81(2): 183-92.

Lai M, Huijbers MG, Lancaster E, Graus F, Bataller L, Balice-Gordon R, *et al.* Investigation of LGI1 as the antigen in limbic encephalitis previously attributed to potassium channels: a case series. Lancet Neurol 2010; 9(8): 776-85.

Lalic T, Pettingill P, Vincent A, Capogna M. Human limbic encephalitis serum enhances hippocampal mossy fiber-CA3 pyramidal cell synaptic transmission. Epilepsia 2011; 52(1): 121-31.

Lovero KL, Fukata Y, Granger AJ, Fukata M, Nicoll RA. The LGI1-ADAM22 protein complex directs synapse maturation through regulation of PSD-95 function. Proc Natl Acad Sci U S A 2015; 112(30): E4129-37.

McKinney RA. Excitatory amino acid involvement in dendritic spine formation, maintenance and remodelling. J Physiol 2010; 588(Pt 1): 107-16.

Mikasova L, P. DR, Bouchet D, Georges F, Rogemond V, Didelot A, *et al.* Disrupted surface cross-talk between NMDA and Ephrin-B2 receptors in anti-NMDA encephalitis. Brain 2012; 135(Pt 5): 1606-21.

Morante-Redolat JM, Gorostidi-Pagola A, Piquer-Sirerol S, Saenz A, Poza JJ, Galan J, *et al.* Mutations in the LGI1/Epitempin gene on 10q24 cause autosomal dominant lateral temporal epilepsy. Hum Mol Genet 2002; 11(9): 1119-28.

Ohkawa T, Fukata Y, Yamasaki M, Miyazaki T, Yokoi N, Takashima H, *et al.* Autoantibodies to epilepsy-related LGI1 in limbic encephalitis neutralize LGI1-ADAM22 interaction and reduce synaptic AMPA receptors. J Neurosci 2013; 33(46): 18161-74.

Owuor K, Harel NY, Englot DJ, Hisama F, Blumenfeld H, Strittmatter SM. LGI1-associated epilepsy through altered ADAM23-dependent neuronal morphology. Mol Cell Neurosci 2009; 42(4): 448-57.

Peng X, Hughes EG, Moscato EH, Parsons TD, Dalmau J, Balice-Gordon RJ. Cellular plasticity induced by anti-alpha-amino-3-hydroxy-5-methyl-4-isoxazolepropionic acid (AMPA) receptor encephalitis antibodies. Ann Neurol 2015; 77(3): 381-98.

Planaguma J, Haselmann H, Mannara F, Petit-Pedrol M, Grunewald B, Aguilar E*, et al.* Ephrin-B2 prevents N-methyl-D-aspartate receptor antibody effects on memory and neuroplasticity. Ann Neurol 2016; 80(3): 388-400.

Planaguma J, Leypoldt F, Mannara F, Gutierrez-Cuesta J, Martin-Garcia E, Aguilar E*, et al.* Human N-methyl D-aspartate receptor antibodies alter memory and behaviour in mice. Brain 2015; 138(Pt 1): 94-109.

Poza JJ, Saenz A, Martinez-Gil A, Cheron N, Cobo AM, Urtasun M*, et al.* Autosomal dominant lateral temporal epilepsy: clinical and genetic study of a large Basque pedigree linked to chromosome 10q. Ann Neurol 1999; 45(2): 182-8.

Sabater L, Planaguma J, Dalmau J, Graus F. Cellular investigations with human antibodies associated with the anti-IgLON5 syndrome. J Neuroinflammation 2016; 13(1): 226.

Schulte U, Thumfart JO, Klocker N, Sailer CA, Bildl W, Biniossek M*, et al.* The epilepsy-linked Lgi1 protein assembles into presynaptic Kv1 channels and inhibits inactivation by Kvbeta1. Neuron 2006; 49(5): 697-706.

Seagar M, Russier M, Caillard O, Maulet Y, Fronzaroli-Molinieres L, De San Feliciano M*, et al.* LGI1 tunes intrinsic excitability by regulating the density of axonal Kv1 channels. Proc Natl Acad Sci U S A 2017; 114(29): 7719-24.

Sirerol-Piquer MS, Ayerdi-Izquierdo A, Morante-Redolat JM, Herranz-Perez V, Favell K, Barker PA*, et al.* The epilepsy gene LGI1 encodes a secreted glycoprotein that binds to the cell surface. Hum Mol Genet 2006; 15(23): 3436-45.

Staub E, Perez-Tur J, Siebert R, Nobile C, Moschonas NK, Deloukas P*, et al.* The novel EPTP repeat defines a superfamily of proteins implicated in epileptic disorders. Trends Biochem Sci 2002; 27(9): 441-4.

van Sonderen A, Petit-Pedrol M, Dalmau J, Titulaer MJ. The value of LGI1, Caspr2 and voltage-gated potassium channel antibodies in encephalitis. Nat Rev Neurol 2017a; 13(5): 290-301.

van Sonderen A, Roelen DL, Stoop JA, Verdijk RM, Haasnoot GW, Thijs RD*, et al.* Anti-LGI1 encephalitis is strongly associated with HLA-DR7 and HLA-DRB4. Ann Neurol 2017b; 81(2): 193-8.

van Sonderen A, Thijs RD, Coenders EC, Jiskoot LC, Sanchez E, de Bruijn MA*, et al.* Anti-LGI1 encephalitis: Clinical syndrome and long-term follow-up. Neurology 2016; 87(14): 1449-56.

Yu YE, Wen L, Silva J, Li Z, Head K, Sossey-Alaoui K*, et al.* Lgi1 null mutant mice exhibit myoclonic seizures and CA1 neuronal hyperexcitability. Hum Mol Genet 2010; 19(9): 1702-11.

Zhou YD, Lee S, Jin Z, Wright M, Smith SE, Anderson MP. Arrested maturation of excitatory synapses in autosomal dominant lateral temporal lobe epilepsy. Nat Med 2009; 15(10): 1208-14.

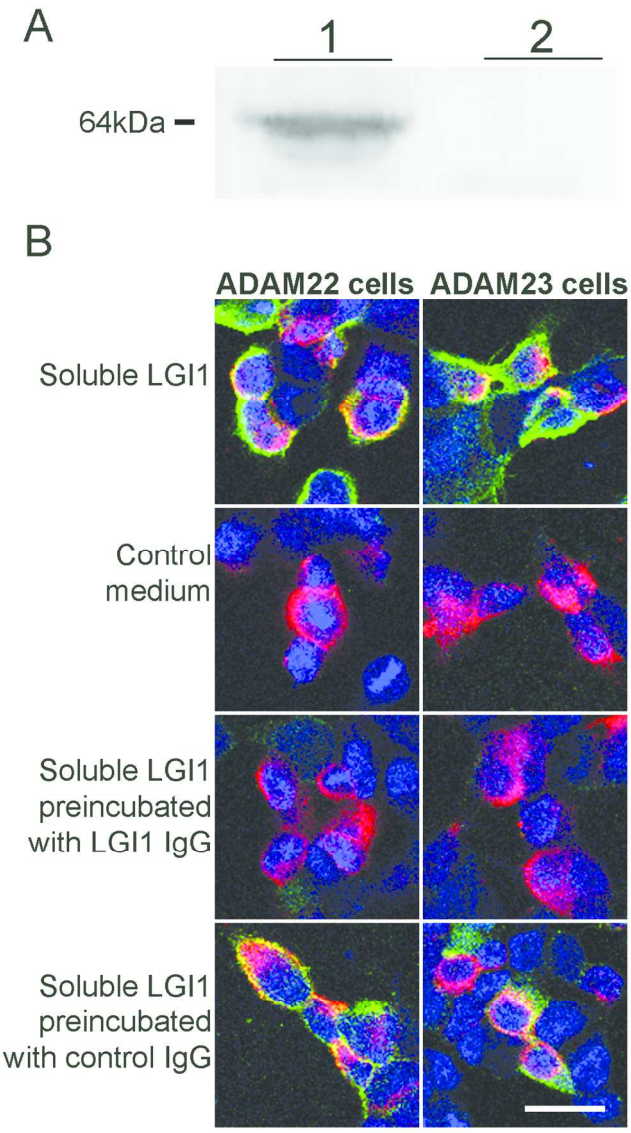

Figure 1: Patient's LGI1 IgG blocks the binding of soluble LGI1 to ADAM22 and ADAM23 The media of HEK293 cells transfected with LGI1 contains secreted LGI1 (A, lane 1) whereas the media of non-transfected cells does not contain LGI1 (A, lane 2). HEK293 cells expressing ADAM22 or ADAM23 bind soluble LGI1 present in the media of HEK293 cells expressing LGI1 (B, first row) but not present in control media (B, second row). When the media with soluble LGI1 is pre-incubated with a representative patient's LGI1 IgG the binding of LGI1 to ADAM22 or ADAM23 is abrogated (B, third row); in contrast, no blocking of the binding is observed when the media is pre-incubated with control IgG (B, fourth row). Scale bar = 20 μm.

90x169mm (300 x 300 DPI)

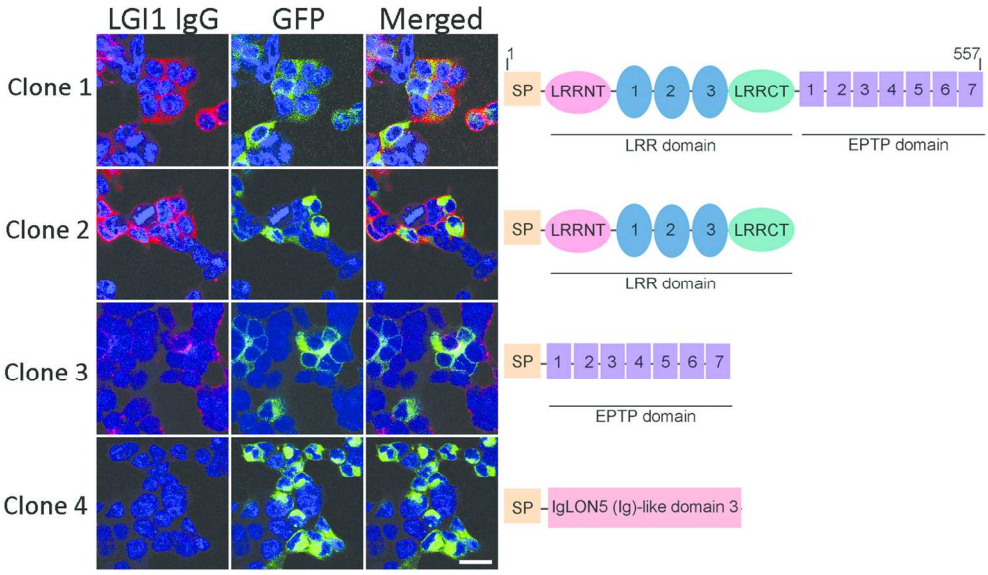

Figure 2: Reactivity of a patient's serum with deletion constructs of LGI1 Serum from a representative patient with anti-LGI1 encephalitis shows predominant reactivity with the full-length sequence of LGI1 (clone 1), and the construct that contains the LRR domain (clone 2); milder reactivity is shown with the construct that contains the EPTP domain (clone 3). The construct generated by clone 4 contains the signal peptide (SP) but does not include any LGI1 sequence. Scale bar = 20 μm.

127x74mm (300 x 300 DPI)

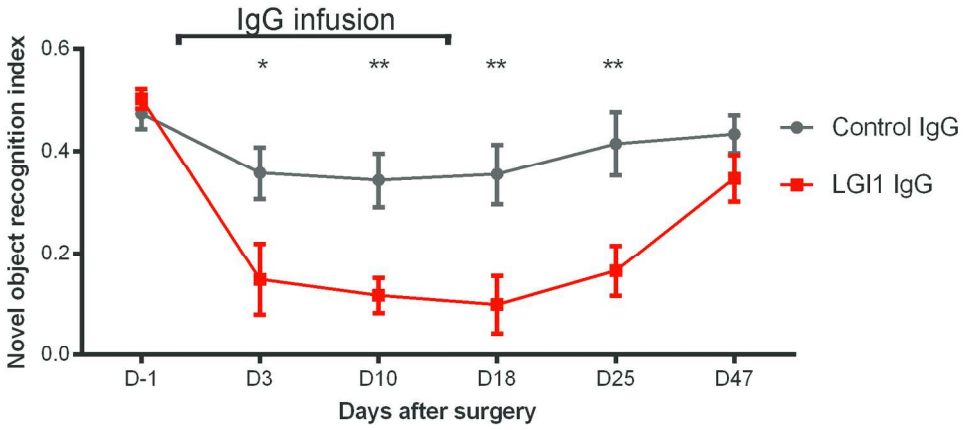

Figure 3: Cerebroventricular infusion of patients' LGI1 IgG causes decrease of memory Novel object recognition index in mice treated with patients' IgG (red, n = 16) or control IgG (grey, n = 14). A high index indicates better memory. Data is presented as mean ± SEM. *P<0.05; **P<0.01.

165x74mm (300 x 300 DPI)

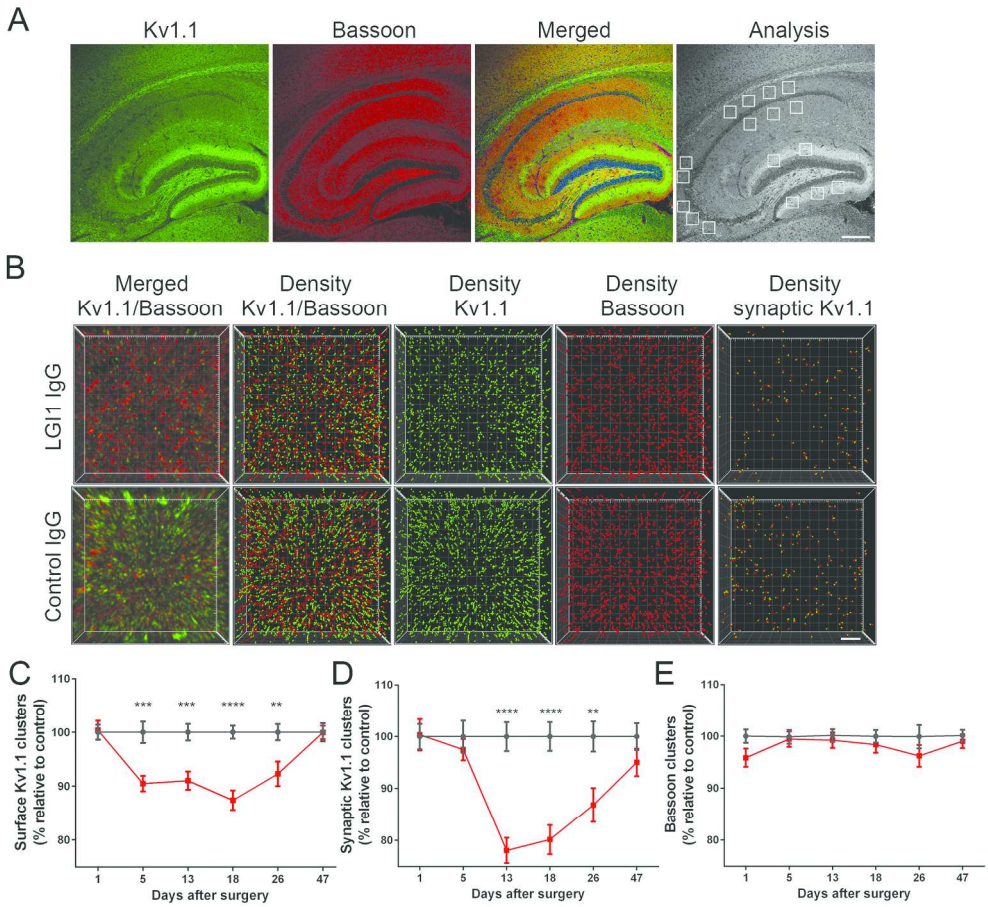

Figure 4: Patients' LG1 IgG causes a decrease of total cell surface and synaptic Kv1.1 clusters in the hippocampus Sagittal section of hippocampus of a representative mouse infused with patients' LGI1 IgG demonstrating the immunostaining of Kv1.1, Bassoon, and the merging reactivities (A). Squares in "Analysis" indicate the analyzed subregions in CA1, CA3, and DG for each animal. Scale bar = 200 µm. 3D projection and analysis of the density of total cell surface clusters of Kv1.1 and Bassoon, and synaptic clusters of Kv1.1 (defined as Kv1.1 clusters that co-localized with Bassoon) in one of the indicated CA3 subregions (A "Analysis"). Merged images (B, left upper and lower squares; Kv1.1 green, and Bassoon red) were post-processed and used to calculate the density of the indicated clusters (density = spots/µm^3). Scale bar = 2 µm. Quantification of the density of total cell surface (C) and synaptic (D) Kv1.1 clusters, and Bassoon clusters (E) in a pooled analysis of hippocampal subregions (CA1, CA3, DG) in animals treated with patients' LGI1 IgG (red) or control IgG (black) on the indicated days. Mean density of clusters in control IgG treated animals was defined as 100%. Data are presented as mean ± SEM. For each time point five animals infused with patients' LGI1 IgG and five with control IgG were examined. Significance of treatment effect was assessed by two-way ANOVA with an alpha-error of 0.05 (asterisks) and post-hoc testing with Sidak-Holm adjustment. ***P*< 0.01; ****P*<0.001; *****P*<0.0001.

199x183mm (300 x 300 DPI)

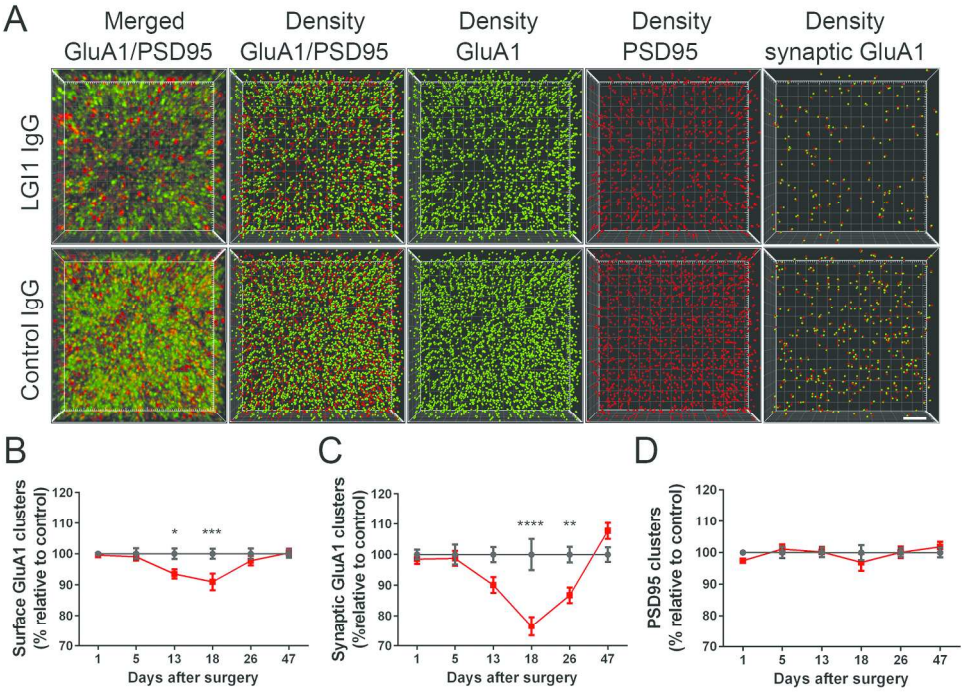

Figure 5: Patients' LG1 IgG causes a decrease of total cell surface and synaptic AMPAR clusters in the hippocampus 3D projection and analysis of the density of total cell surface clusters of GluA1 AMPAR and PSD95, and synaptic clusters of AMPAR (defined as AMPAR clusters that co-localized with PSD95) in one of the CA3 subregions indicated in Fig. 4A, "Analysis". Merged images (A, left upper and lower squares; GluA1 green, and PSD95 red) were post-processed and used to calculate the density of the indicated clusters (density = spots/μm^3). Scale bar = 2 µm. Quantification of the density of total cell surface (B) and synaptic (C) GluA1 AMPAR clusters, and PSD95 clusters (D) in a pooled analysis of hippocampal subregions (CA1, CA3, DG) in animals treated with patients' LGI1 IgG (red) or control IgG (black) on the indicated days. Mean density of clusters in control IgG treated animals was defined as 100%. Data are presented as mean ± SEM. For each time point five animals infused with patients' IgG and five with control IgG were examined. Significance of treatment effect was assessed by two-way ANOVA with an alpha-error of 0.05 (asterisks) and post-hoc testing with Sidak-Holm adjustment. *P< 0.05; **P< 0.01; ***P<0.001; ****P<0.0001.

199x147mm (300 x 300 DPI)

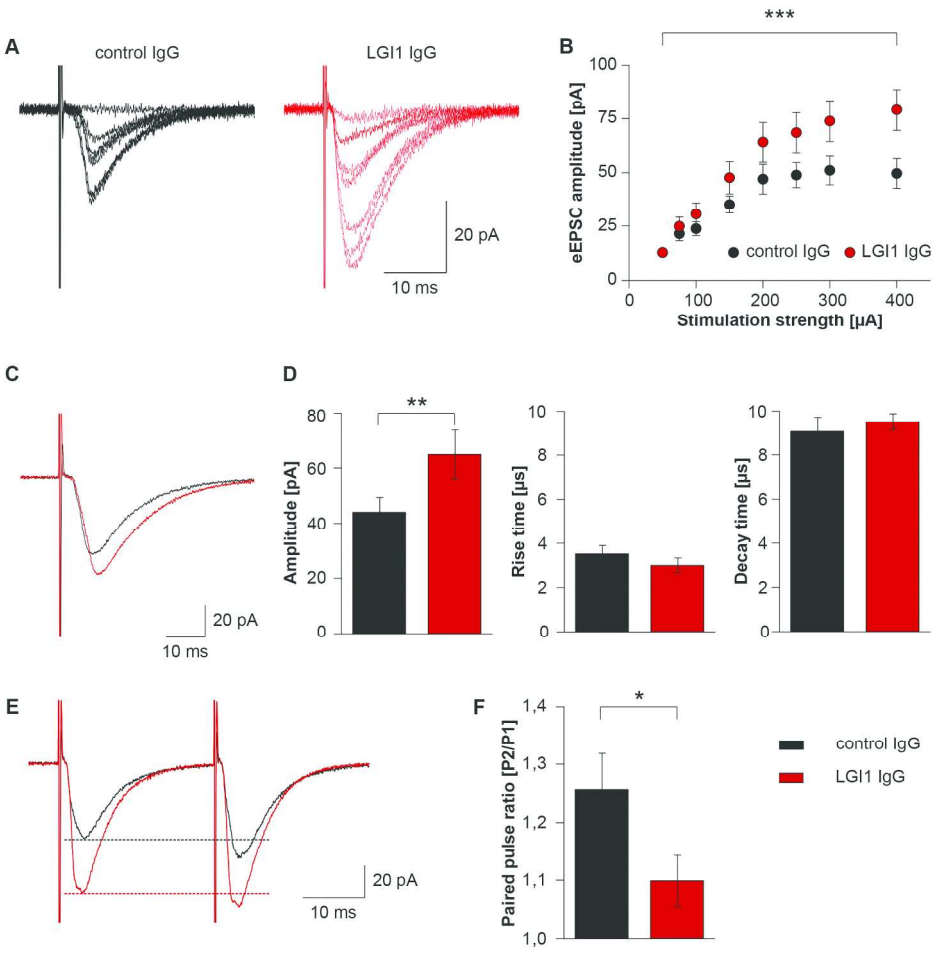

Figure 6: Patients'LGI1 IgG increases excitatory synaptic transmission Evoked excitatory postsynaptic currents (eEPSCs) in dentate gyrus granule cells upon incremental stimulation of medial perforant path (MPP) afferent fibers are increased in acute brain slices of mice that received patient´s LGI1 IgG (A and B). Example traces of an individual recording are shown in (A). In/out characteristics of granule cell neurons of control IgG and patients' LGI1 IgG treated mice (B; $n_{control\ IgG}$ = 13; $n_{LGI1\ IgG}$ = 15; data are presented as mean ± SEM; two-way ANOVA and Holm-Sidak post-hoc test. ***P<0.001). Peak amplitude of eEPSCs (example traces in C) is increased after infusion of antibodies against LGI1, whereas rise and decay time is unchanged ($n_{control\ IgG}$ = 13; $n_{LGI1\ IgG}$ = 15; data are presented as mean ± SEM; unpaired t-test. **P<0.01) (C and D). Paired pulse facilitation with an interstimulus interval of 50 ms is reduced in granule cell neurons from mice after infusion of patients' LGI1 IgG indicating increased release probability. Example traces in E; dashed lines indicate peak amplitude of the first pulse ($n_{control\ IgG}$ = 11; $n_{LGI1\ IgG}$ = 13; data are presented as mean ± SEM; unpaired t-test. *P<0.05) (E and F).

204x195mm (300 x 300 DPI)

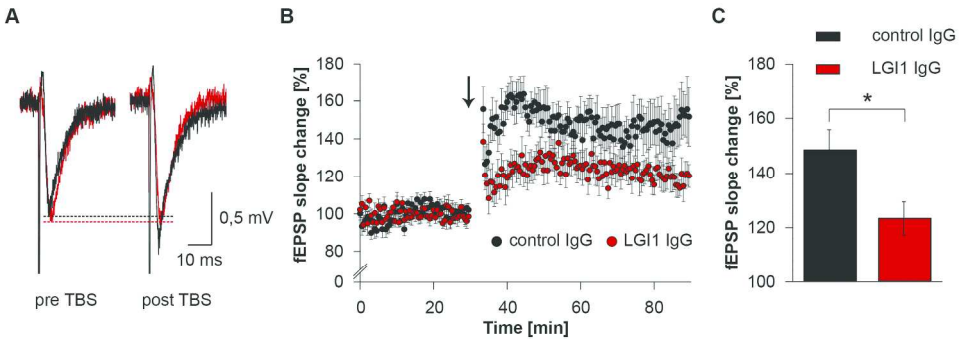

Figure 7: Patients' LGI1 IgG alters synaptic plasticity Example traces of individual field excitatory postsynaptic potential (fEPSP) recordings in the CA1 region before and after theta burst stimulation (TBS) of Schaffer collateral afferents show reduced fEPSP potentiation in brain slices of mice that received patient´s LGI1 IgG (A). Time course and quantitative analysis of long-term potentiation (LTP) after TBS (arrow), demonstrates persistent reduction of fEPSP slope values in slices of mice after infusion of patient´s LGI1 IgG indicating disturbed synaptic plasticity. Quantification of fEPSP slope change is decreased in LGI1 IgG infused mice (B and C, $n_{control\ IgG}$ = 10; $n_{LGI1\ IgG}$ = 13; data are presented as mean ± SEM; unpaired t-test. *P<0.05).

206x73mm (300 x 300 DPI)

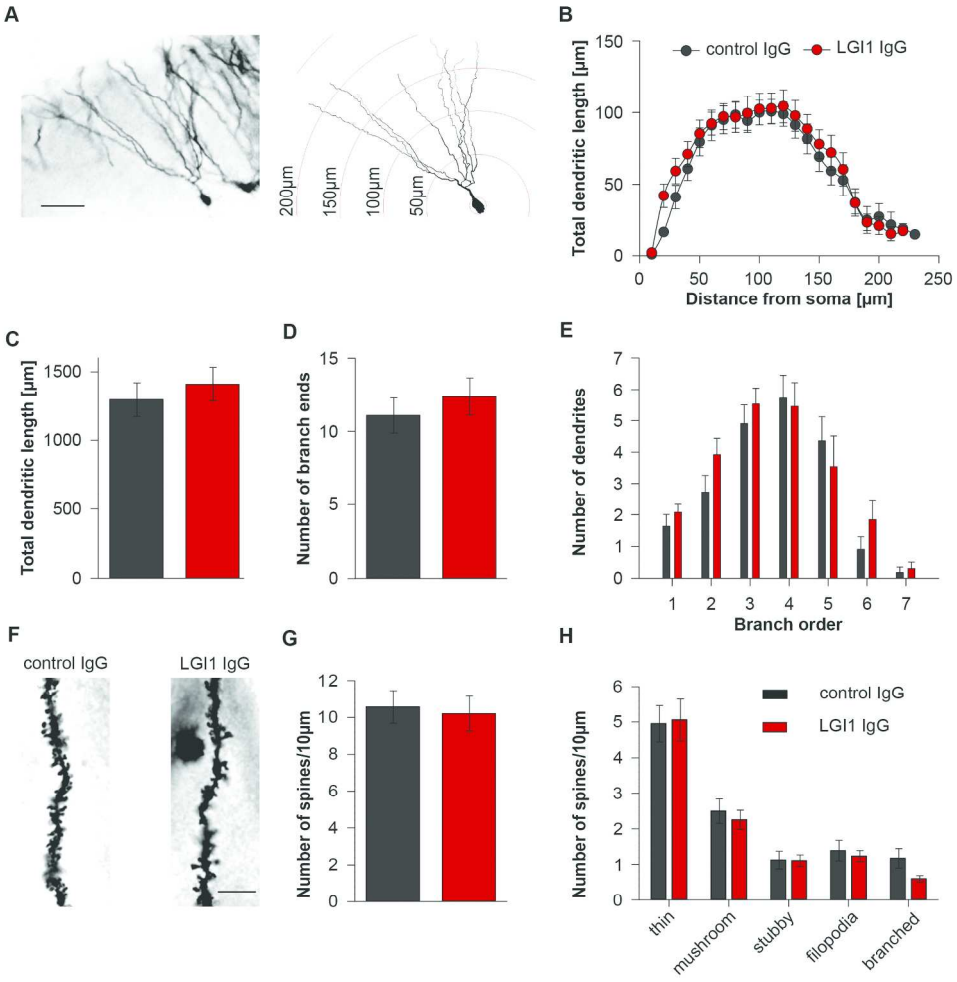

Figure 8: Dendritic pruning is unaffected by patients' LGI1 IgG Dendritic arborization of a dentate gyrus granule cell; example neuron is shown after Golgi silver impregnation (left) and in Neurolucida reconstruction for Sholl analysis (right) (A, scale bar = 50 µm). Sholl analysis revealed unchanged dendritic arborization in control IgG and patients' LGI1 IgG infused mice as shown by the length of hippocampal granule cell dendrites (B and C) and by number and intersection of dendritic branches (D and E). Synaptic spines of tertiary dendrites of CA1 pyramidal neurons (F, scale bar = 10µm). Quantification of spine density (G) and of spine morphology (H) is unchanged in control IgG and patients' LGI1 IgG infused mice (all data are presented as mean ± SEM).

203x203mm (300 x 300 DPI)

Supplementary material

- Immunoblot of soluble LGI1
- Mice, surgery, placement of ventricular catheters and osmotic pumps
- Behavioral tasks
- Golgi-Cox staining
- Sholl analysis
- Supplementary Table 1
- Supplementary Figure 1: Immunoabsorption of patients' purified IgG with LGI1-expressing HEK293 cells
- Supplementary Figure 2: LGI1 IgG isolated from patients' serum does not react with brain of LGI1 null mice
- Supplementary Figure 3: Distribution of behavioral tests, period of infusion, and brain tissue studies
- Supplementary Figure 4: Patients' LGI1 IgG blocks the binding of LGI1 to ADAM23 more frequently than to ADAM22
- Supplementary Figure 5: Tests of anxiety, aggression, and locomotor activity
- Supplementary Figure 6: Presence of patients' antibodies bound to LGI1 in brain of infused mice

Immunoblot of soluble LGI1

Media from the indicated LGI1-expressing HEK293 cells, and media from non-transfected cells, were normalized in protein concentration, and 100 µg of protein diluted 1:2 with Rotiload (#K929.1, Roth) boiled for 5 minutes, and separated in a 10% polyacrylamide gel electrophoresis. After transferring the proteins to a PVDF membrane, they were probed with a monoclonal rabbit antibody against LGI1 (1:200, #ab30868, Abcam) for 2 hours at 4°C, and the reactivity developed using the avidin-biotin immunoperoxidase method.

Mice, surgery, placement of ventricular catheters and osmotic pumps

Male C57BL6/J mice (Charles River), 8-10 weeks old (25-30 grams) were housed in cages of five until one week before surgery when they were housed individually. The room was maintained at a controlled temperature (21±1ºC) and humidity (55±10%) with

illumination at 12-hour cycles; food and water were available *ad libitum*. All experiments were performed during the light phase, and animals were habituated to the experimental room for 1 week before starting the tests.

Cerebroventricular infusion of patients' LGI1 IgG or control IgG was performed using osmotic pumps (model 1002, Alzet, Cupertino, CA) with the following characteristics: volume 100 µl, flow rate 0.25 µl/hour, and duration 14 days, as reported (Planaguma *et al.*, 2015). In brief, 24 hours before surgery, two osmotic pumps per animal were each loaded with 100 µl of purified patients' LGI1 IgG or control IgG (1µg/µl). Mice were then placed in a stereotaxic frame, and a bilateral cannula (model 3280PD-2.0/SP, PlasticsOne) was inserted into the ventricles (coordinates: 0.2 mm posterior and ±1.00 mm lateral from bregma, depth 2.2 mm), as reported (Planaguma *et al.*, 2015). Each arm of the cannula was connected to one osmotic pump, which was subcutaneously implanted on the back of the mice (two pumps per animal). Appropriate ventricular placement of the catheters was assessed in randomly selected mice injecting methylene blue through the catheters, as reported (Planaguma *et al.*, 2015).

Behavioral tasks

Multiple behavioral tasks were applied at different time points related to the day of pump implantation and initiation of the ventricular infusion of patients' LGI1 IgG or control IgG. They included the novel object recognition (NOR) index and spontaneous locomotor activity (LOC), which were tested 1 day before surgery and on days 3, 10, 18, 25 and 47 after surgery, black and white test (BW, day 7), elevated plus maze (EPM, day 17), and resident-intruder test (RI, days 11 and 26). The distribution of behavioral tests in relation to the infusion period is shown in Supplementary Fig. 3.

Detailed information on these tests has been previously reported (Planaguma *et al.*, 2015).

Golgi-Cox staining

Golgi silver impregnation was conducted with the FD Rapid GolgiStainTM Kit (#PK401, FD NeuroTechnologies, Inc., Columbia, USA) according to manufacturer's instructions. Briefly, the tissue was rinsed in aCSF1 to remove blood residues, and was then transferred into equal amounts of solution A+B of the FD Rapid GolgiStainTM Kit. After renewal of solutions on the second day the tissue was subsequently left in the dark for two weeks at room temperature. Thereafter, brain hemispheres were transferred into solution C of the FD Rapid GolgiStainTM Kit, which was changed after one day, and were left in solution at 4°C for 5 days. Hemispheres were then stored at -80°C until further use. Thereafter, hemispheres were cut into 150µm thick coronal slices in the area of the hippocampus using a Leica CM3050S cryostat and mounted on object slides. For the last step of staining procedure, slices were washed in purified water (2 x 4 minutes), incubated in a mix of 1/4 solution D, 1/4 solution E and 1/2 purified water for 10 minutes, washed again, and then dehydrated in an ascending alcohol series (50%, 75%, 95% for 4 minutes each, and 2 x 100 % for 8 minutes). Finally, slices were immersed in xylene (2 x 5 minutes), and then quickly coverslipped with Entellan® (Merck KGaG, Darmstadt, Germany) and dehumidified overnight.

Sholl analysis

To evaluate dendritic morphology, a Zeiss Axioskop 2 mot plus (Zeiss, Oberkochen, Germany) and a computer-based system (Neurolucida; MicroBrightField) was used to generate three-dimensional neuron tracings that were subsequently analyzed using the

NeuroExplorer Software (MicroBrightField). Golgi-impregnated cells were selected for reconstruction if they fulfilled the following criteria: (1) the neuron was located in the dentate gyrus with soma in outer granule layer of the superior or inferior blade, (2) the neuron was distinguishable from neighboring cells to allow for identification of dendrites, (3) the dendrites were not truncated or broken, and (4) the cell exhibited dark and well filled impregnation throughout whole dendrites including spines. Selected cells were traced manually using the Neurolucida system at 40x magnification. For each reconstructed neuron an estimate of dendritic complexity was obtained using the Sholl ring method (Zhou *et al*., 2009). Additionally, the total dendritic length, the number of branch ends and the number of dendrites per branch order were calculated.

For analysis of dendritic spines, positively stained neurons in the CA region were randomly selected and used for analysis as described previously (Orlowski and Bjarkam, 2012). Neuronal apical dendrites were followed up to tertiary branches without visible disruptions and without further split up using a Zeiss Axioskop 2 mot plus with a 100x oil immersion objective (PLAN-Neofluar). For correct analysis of dendrite length, tertiary branches were chosen to be in an even z-layer. Number and type of spines (thin, mushroom, stubby, filopodia or branched) were counted manually by the same blinded investigator according to previous reports (McKinney, 2010). Total spine density was calculated as number of spines per 10 µm of dendritic length. Morphological subclassification was outlined in proportion of all spines regardless of spine properties.

Supplementary Table 1: Patients clinical and immunological features

Patient	Age	Gender	Main clinical syndrome	Facio-brachial dystonic seizures	Other seizure types	MRI T2/ FLAIR increased signal	Clones reactivity	Blocking with ADAM23	Blocking with ADAM22
1	62	F	Limbic encephalitis	No	Generalized	No	LRR	Yes	No
2	54	F	Limbic encephalitis	Yes	No	Unilateral mesiotemporal	LRR	Yes	Yes
3	73	M	Limbic encephalitis	Yes	No	No	LRR	Yes	Yes
4	65	M	Limbic encephalitis	No	Generalized	Unilateral mesiotemporal	LRR, EPTP	Yes	Yes
5	65	M	Limbic encephalitis	No	Focal	Bilateral mesiotemporal	LRR	Yes	No
6	63	F	Limbic encephalitis	No	Focal and generalized	Bilateral mesiotemporal	LRR, EPTP	Yes	No
7	52	F	Limbic encephalitis	No	Generalized	Bilateral mesiotemporal	LRR	Yes	No
8	59	M	Limbic encephalitis	Yes	Focal and generalized	Basal ganglia, frontal, insula	LRR	Yes	Yes
9	71	F	Limbic encephalitis	Yes	Focal and generalized	No	LRR	Yes	Yes
10	57	M	Limbic encephalitis	No	Focal and generalized	Bilateral mesiotemporal	LRR, EPTP	Yes	No
11	63	M	Limbic encephalitis	Yes	Focal and generalized	Bilateral mesiotemporal	LRR, EPTP	Yes	Yes
12	72	M	Limbic encephalitis	Yes	No	Unilateral mesiotemporal sclerosis	LRR, EPTP	Yes	No
13	80	M	Limbic encephalitis	No	Focal	No	LRR	Yes	No
14	71	F	Limbic encephalitis	No	Generalized	Bilateral mesiotemporal	LRR, EPTP	Yes	Yes
15	61	M	Limbic encephalitis	No	Focal and generalized	Bilateral mesiotemporal	LRR, EPTP	Yes	Yes

						and basal ganglia			
16	74	M	Limbic encephalitis	Yes	Focal	Bilateral mesiotemporal	LRR, EPTP	Yes	Yes
17	59	M	Limbic encephalitis	Unknown	Focal and generalized	No	LRR	Yes	No
18	56	M	Limbic encephalitis	No	Focal	Unilateral mesiotemporal	LRR	Yes	No
19	54	F	Limbic encephalitis	Unknown	NA	Bilateral mesiotemporal	LRR, EPTP	Yes	Yes
20	58	M	Limbic encephalitis	No	No	Bilateral mesiotemporal	LRR, EPTP	Yes	Yes
21	65	M	Limbic encephalitis	Yes	Focal and generalized	Unilateral insula	LRR	Yes	Yes
22	41	M	Limbic encephalitis	Yes	Focal	No	LRR	Yes	Yes
23	56	M	Limbic encephalitis	Unknown	Focal	Unilateral mesiotemporal	LRR	Yes	No
24	53	F	Limbic encephalitis	Yes	Focal	No	LRR, EPTP	Yes	Yes
25	58	F	Limbic encephalitis	Yes	Focal	Bilateral mesiotemporal	LRR, EPTP	Yes	Yes

Supplementary figures

Supplementary Figure 1: Immunoabsorption of patients' purified IgG with LGI1-expressing HEK293 cells

Reactivity of patients' LGI1 IgG with rat brain (A), HEK293 cells that express LGI1 (B) and live cultures of neuron (C). Pre-absorption of patients'LGI1 IgG with HEK293 cells expressing LGI1 abolished the reactivity in all three conditions (D, E, F). In contrast, pre-absorption with HEK293 cells without LGI1 did not alter the reactivity in the three indicated conditions (G, H, I). Scale bar in G = 2 mm; Scale bar in H = 20 μm; Scale bar in I = 50 μm.

Supplementary Figure 2: LGI1 IgG isolated from patients' serum does not react with brain of LGI1 null mice

Purified LGI1 IgG from patients intensively reacts with hippocampus of wild type mice but it does not react with hippocampus of LGI1 null mice (tissue obtained as reported, (Lai *et al.*, 2010)). Purified IgG from healthy participants (control) does not show reactivity with any of the brains. Scale bar = 200 μm.

Supplementary Figure 3: Distribution of behavioral tests, period of infusion, and brain tissue studies

At day 0, catheters and osmotic pumps were placed and bilateral ventricular infusion of patients' LGI1 IgG or control IgG started. Infusion lasted for 14 days. Memory (novel object recognition [NOR]), locomotor activity (LOC), anxiety (black and white test [BW] and elevated plus maze test [EPM]), and aggressiveness (resident intruder test [RI]) were assessed blinded to treatment at the indicated days. Animals were habituated

for 1 to 4 days before surgery (baseline) to NOR and LOC. Red arrowheads indicate the days of sacrifice for studies of effects of antibodies in brain.

Supplementary Figure 4: Patients' LGI1 IgG blocks the binding of LGI1 to ADAM23 more frequently than to ADAM22

Sera from four additional representative patients show that all block the binding of LGI1 to ADAM23, but two of them (serum 3 and 4) do not block the binding of LGI1 to ADAM22. Scale bar = 20 μm.

Supplementary Figure 5: Tests of anxiety, aggression, and locomotor activity

Tests of anxiety (black and white test, A, and elevated plus maze, B), aggression (resident intruder, C), and locomotor activity (D) did not show significant differences between mice infused with patients' LGI1 IgG and control (CT) IgG. B entries = black entries; W entries = white entries; CA entries = closed arm entries; OA = open arm entries. D = day of the experiment related to first day of IgG infusion; Hab = habituation.

Supplementary Figure 6: Presence of patients' antibodies bound to LGI1 in brain of infused mice

In mice infused with patients' LGI1 IgG (A, lanes 1 and 2), but not in mice infused with control IgG (A, lanes 3 and 4), the extraction and precipitation of IgG from brain show that it is bound to LGI1 (64 kDa protein band in lanes 1 and 2).

In another experiment, acid-extracted IgG from hippocampus of mice infused with patients' IgG shows the presence of LGI1 antibodies, which are demonstrated in a cell-

based assay with HEK293 cells expressing LGI1 (first row in B). In contrast no LGI1 antibodies are detected in the tissue-wash before the acid extraction (second row) suggesting the acid-extracted IgG contained antibodies specifically bound to LGI1 in tissue. Similar experiments with samples obtained from mice infused with control IgG show absence of LGI1 antibodies (third and fourth rows). For all rows the expression of LGI1 in HEK293 cells was confirmed with a monoclonal rabbit antibody against LGI1 (1:1000, #ab30868, Abcam) showing the merged reactivities of the human and monoclonal antibodies. Scale bar = 20 μm.

Supplementary References

Lai M, Huijbers MG, Lancaster E, Graus F, Bataller L, Balice-Gordon R, *et al.* Investigation of LGI1 as the antigen in limbic encephalitis previously attributed to potassium channels: a case series. Lancet Neurol 2010; 9(8): 776-85.

McKinney RA. Excitatory amino acid involvement in dendritic spine formation, maintenance and remodelling. J Physiol 2010; 588(Pt 1): 107-16.

Orlowski D, Bjarkam CR. A simple reproducible and time saving method of semi-automatic dendrite spine density estimation compared to manual spine counting. J Neurosci Methods 2012; 208(2): 128-33.

Planaguma J, Leypoldt F, Mannara F, Gutierrez-Cuesta J, Martin-Garcia E, Aguilar E, *et al.* Human N-methyl D-aspartate receptor antibodies alter memory and behaviour in mice. Brain 2015; 138(Pt 1): 94-109.

Zhou YD, Lee S, Jin Z, Wright M, Smith SE, Anderson MP. Arrested maturation of excitatory synapses in autosomal dominant lateral temporal lobe epilepsy. Nat Med 2009; 15(10): 1208-14.

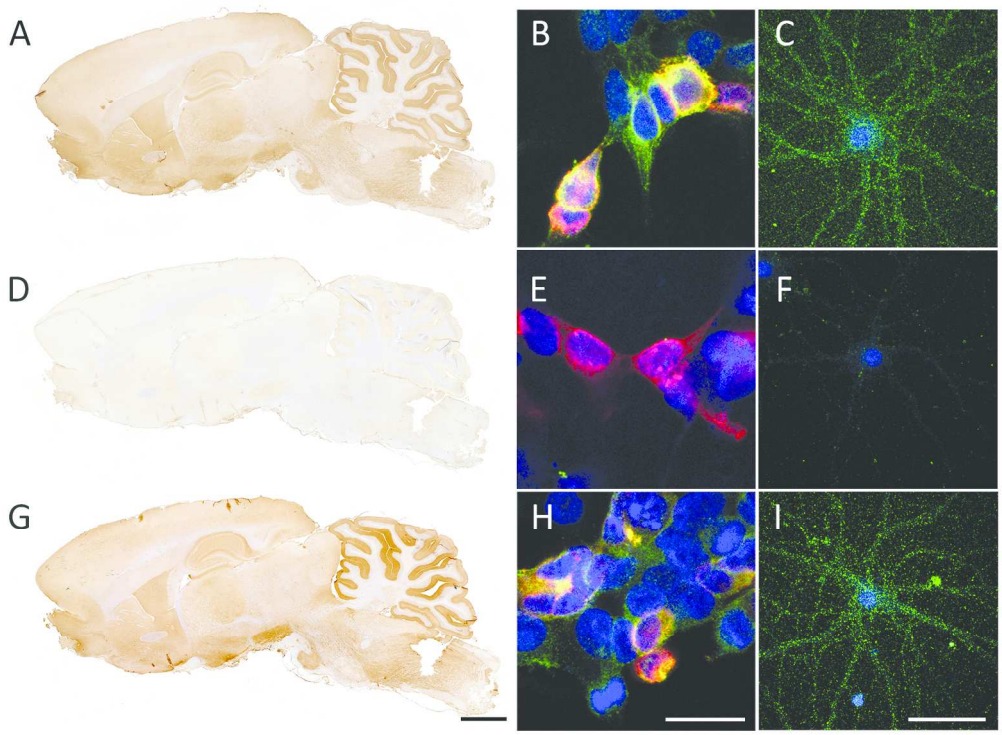

Supplementary Figure 1: Immunoabsorption of patients' purified IgG with LGI1-expressing HEK293 cells Reactivity of patients' LGI1 IgG with rat brain (A), HEK293 cells that express LGI1 (B) and live cultures of neuron (C). Pre-absorption of patients'LGI1 IgG with HEK293 cells expressing LGI1 abolished the reactivity in all three conditions (D, E, F). In contrast, pre-absorption with HEK293 cells without LGI1 did not alter the reactivity in the three indicated conditions (G, H, I). Scale bar in G = 2 mm; Scale bar in H = 20 µm; Scale bar in I = 50 µm.

184x137mm (300 x 300 DPI)

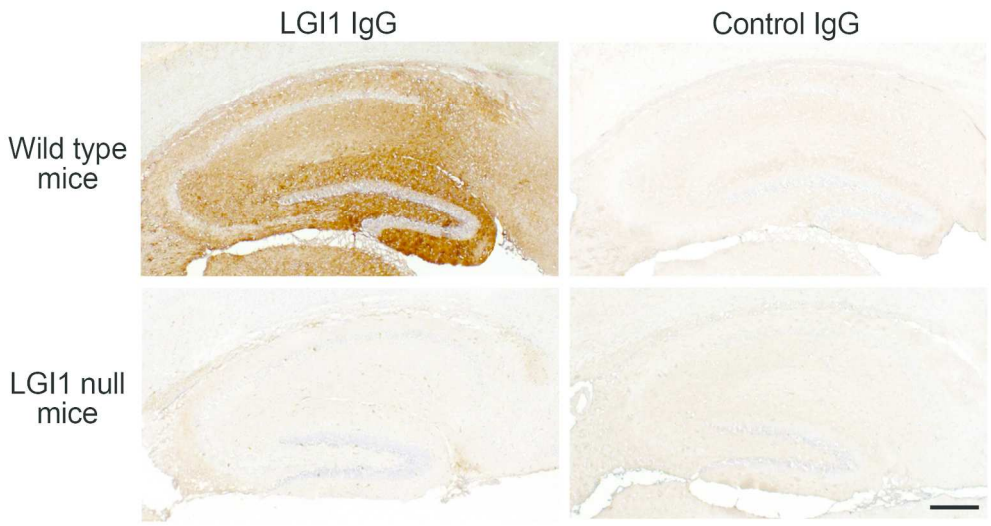

Supplementary Figure 2: LGI1 IgG isolated from patients' serum does not react with brain of LGI1 null mice Purified LGI1 IgG from patients intensively reacts with hippocampus of wild type mice but it does not react with hippocampus of LGI1 null mice (tissue obtained as reported, (Lai et al., 2010)). Purified IgG from healthy participants (control) does not show reactivity with any of the brains. Scale bar = 200 μm.

184x99mm (300 x 300 DPI)

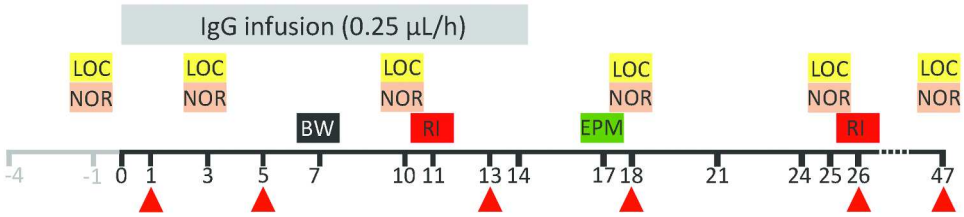

Supplementary Figure 3: Distribution of behavioral tests, period of infusion, and brain tissue studies At day 0, catheters and osmotic pumps were placed and bilateral ventricular infusion of patients' LGI1 IgG or control IgG started. Infusion lasted for 14 days. Memory (novel object recognition [NOR]), locomotor activity (LOC), anxiety (black and white test [BW] and elevated plus maze test [EPM]), and aggressiveness (resident intruder test [RI]) were assessed blinded to treatment at the indicated days. Animals were habituated for 1 to 4 days before surgery (baseline) to NOR and LOC. Red arrowheads indicate the days of sacrifice for studies of effects of antibodies in brain.

199x54mm (300 x 300 DPI)

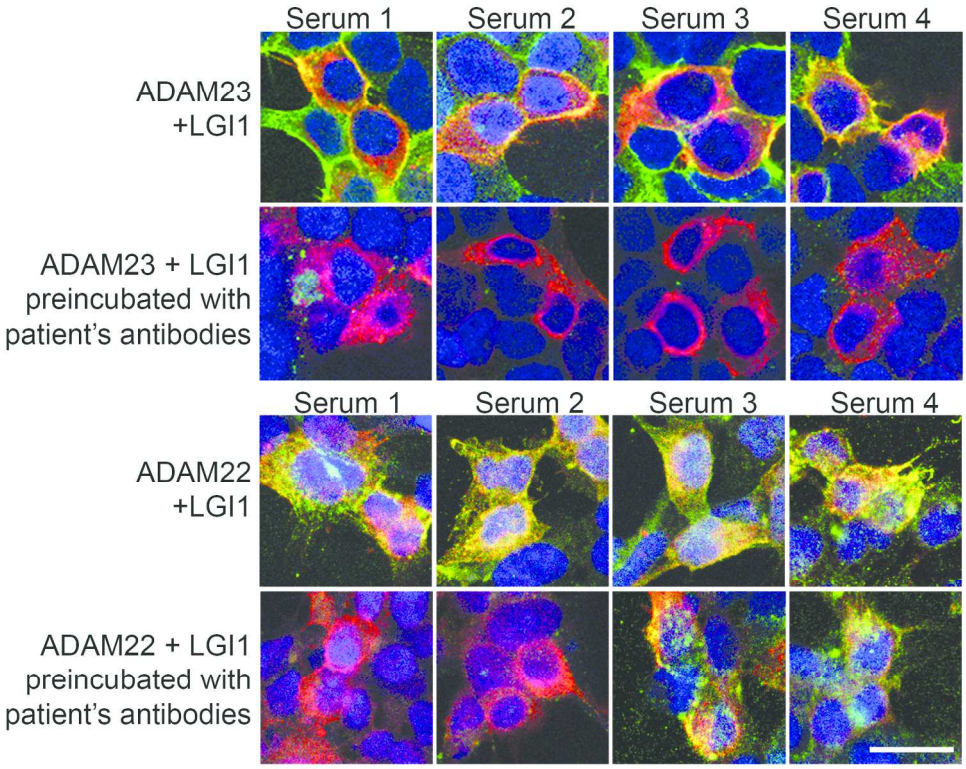

Supplementary Figure 4: Patients' LGI1 IgG blocks the binding of LGI1 to ADAM23 more frequently than to ADAM22 Sera from four additional representative patients show that all block the binding of LGI1 to ADAM23, but two of them (serum 3 and 4) do not block the binding of LGI1 to ADAM22. Scale bar = 20 µm.

184x144mm (300 x 300 DPI)

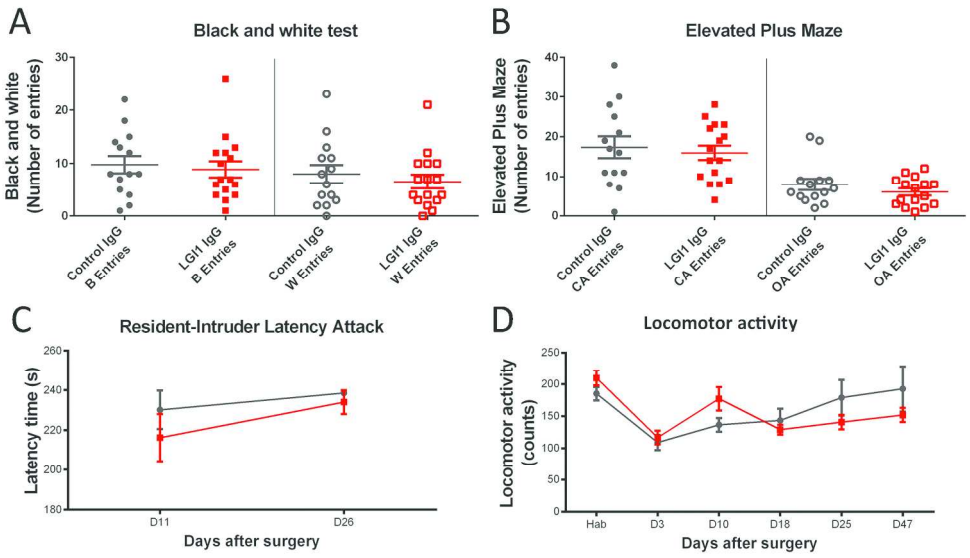

Supplementary Figure 5: Tests of anxiety, aggression, and locomotor activity Tests of anxiety (black and white test, A, and elevated plus maze, B), aggression (resident intruder, C), and locomotor activity (D) did not show significant differences between mice infused with patients' LGI1 IgG and control (CT) IgG. B entries = black entries; W entries = white entries; CA entries = closed arm entries; OA = open arm entries. D = day of the experiment related to first day of IgG infusion; Hab = habituation.

199x112mm (300 x 300 DPI)

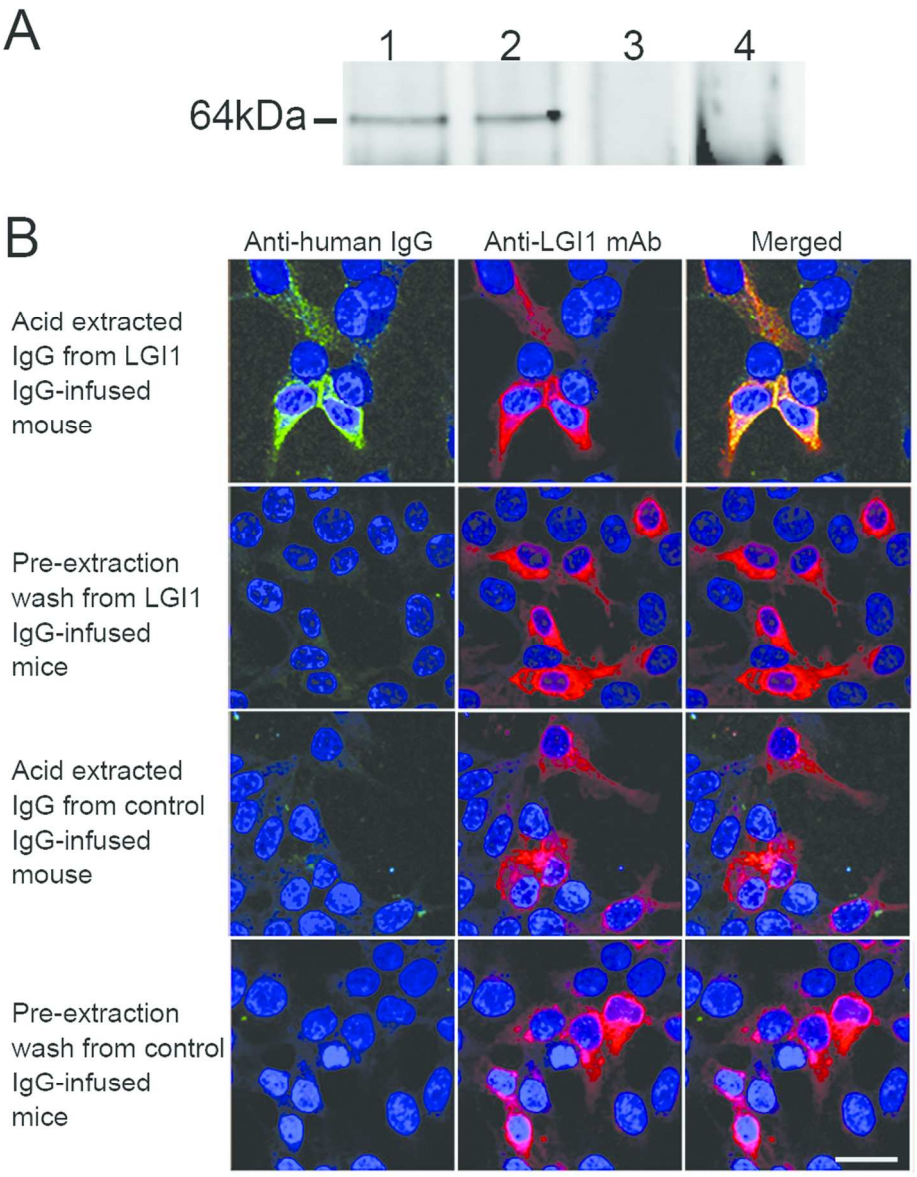

Supplementary Figure 6: Presence of patients' antibodies bound to LGI1 in brain of infused mice
In mice infused with patients' LGI1 IgG (A, lanes 1 and 2), but not in mice infused with control IgG (A, lanes 3 and 4), the extraction and precipitation of IgG from brain show that it is bound to LGI1 (64 kDa protein band in lanes 1 and 2). In another experiment, acid-extracted IgG from hippocampus of mice infused with patients' IgG shows the presence of LGI1 antibodies, which are demonstrated in a cell-based assay with HEK293 cells expressing LGI1 (first row in B). In contrast no LGI1 antibodies are detected in the tissue-wash before the acid extraction (second row) suggesting the acid-extracted IgG contained antibodies specifically bound to LGI1 in tissue. Similar experiments with samples obtained from mice infused with control IgG show absence of LGI1 antibodies (third and fourth rows). For all rows the expression of LGI1 in HEK293 cells was confirmed with a monoclonal rabbit antibody against LGI1 (1:1000, #ab30868, Abcam) showing the merged reactivities of the human and monoclonal antibodies. Scale bar = 20 μm.

90x114mm (300 x 300 DPI)